EUROPEAN UROLOGY 77 (2020) 457–468

available at www.sciencedirect.com
journal homepage: www.europeanurology.com

European Association of Urology

Surgery in Motion

Multiparametric Magnetic Resonance Imaging for the Detection of Clinically Significant Prostate Cancer: What Urologists Need to Know. Part 1: Acquisition

Rianne R.M. Engels[a], *Bas Israël*[a], *Anwar R. Padhani*[b], *Jelle O. Barentsz*[c,*]

[a] *Radboud University Nijmegen Medical Center, Nijmegen, The Netherlands;* [b] *Paul Strickland Scanner Centre, Mount Vernon Hospital, Northwood, UK;* [c] *Department of Radiology, Radboud University Nijmegen Medical Center, Nijmegen, The Netherlands*

Article info

Article history:
Accepted September 11, 2019

Associate Editor:
Alexandre Mottrie

Keywords:
Prostate cancer
Magnetic resonance imaging
Acquisition

EU ★ ACME
www.eu-acme.org/europeanurology

Please visit www.eu-acme.org/europeanurology to answer questions on-line. The EU-ACME credits will then be attributed automatically.

Please visit www.europeanurology.com and www.urosource.com to view the accompanying video.

Abstract

Background: Acquiring multiparametric magnetic resonance images of the prostate is not a simple "push-button" approach.
Objective: To show how image acquisition of prostate multiparametric Magnetic Resonance Imaging (mpMRI) can be optimized.
Design, setting, and participants: Image protocols, magnetic field strength choice, and the use of receiver coils are discussed. In addition, patient preparation and the recognition, prevention, and mitigation of artifacts are evaluated.
Surgical procedure: Based on expert prostate MRI technologists (MRI radiographers) opinion, the optimal protocol is reviewed, and potential artifacts are determined.
Measurements: The entire acquisition process is presented from initial patient preparation until the end of the imaging. The choice of the used equipment, pulse sequences, and prevention of patient- and imaging-related artifacts are presented. This will be shown in individual patients.
Results and limitations: Although the Prostate Imaging Reporting and Data System guidelines (2012 and 2016) describe minimal and optimal acquisition protocols for prostate mpMRI, these standards are not always met in daily practice. A major challenge in mpMRI is to obtain high image quality and reduce its variability for radiologic interpretations. A summary of evidence and guidelines for the acquisition of mpMRI of the prostate can set a basic guideline to reduce these variabilities.
Conclusions: This article and an accompanying video can be used as a guide by MRI technologists (MRI radiographers) to improve their image acquisitions by optimizing protocols, magnetic field strength choice, and use of receiver coils. We also discuss patient preparation and the recognition, prevention, and mitigation of artifacts.
Patient summary: In this first surgery-in-motion contribution, we will show how optimized image acquisition is performed to detect prostate cancer. Both MRI-dependent and patient related factors are discussed.

* Corresponding author. Department of Radiology, Radboud University Nijmegen Medical Center, P.O. Box 9101, Nijmegen, The Netherlands. Tel.: +31 243 619196; Fax: +31 243 540866.
E-mail address: jelle.barentsz@radboudumc.nl (J.O. Barentsz).

https://doi.org/10.1016/j.eururo.2019.09.021

Check for updates

1. Introduction

The success of multiparametric magnetic resonance imaging (mpMRI) for reliably detecting and localizing clinically significant (cs) prostate cancer (PCa) is highly dependent on image quality [1–4]. However, due to the variability of available MRI equipment including software levels and prostate MRI technologists' (MRI radiographers') experience, it can be challenging to consistently achieve good-quality images for detection, localization, staging, and follow-up of PCa.

The first step to improve quality and reduce variability is to implement optimized acquisition protocols. Therefore, the European Society of Urogenital Radiology (ESUR) published the Prostate Imaging Reporting and Data System (PI-RADS) guidelines in 2012, which included recommendations on minimal and optimal requirements for prostate mpMRI. In 2016, this was revised, and more recently PI-RADS v2.1 was published [5–7]. However, these requirements are only technical specifications, and did not describe patient preparation or how to avoid the most common artifacts that are known to affect image quality, which are described herein.

2. Magnetic field strength

One of the most frequently discussed topics of prostate mpMRI is whether to use 1.5T or 3T MRI field strength. The use of 3T machines is recommended [6]. MRI of 1.5T field strength should be considered when a patient has an MR-conditional implanted device, but its presence still may result in artifacts that could compromise image quality (eg, metallic hip-prosthesis) [6].

The reason for 3T MRI being preferred to 1.5T MRI is the increased "signal-to-noise ratio" (SNR), which results in increased spatial resolution and thus better image quality. The disadvantage of 3T MRI is the increased risk of artifacts, especially susceptibility (resulting in geometric distortion) and ghosting artifacts [8]. There are sequences that decrease these artifacts, but these can result in increased imaging time and/or decreased SNR.

A comparison between the 1.5T and 3T MRI by Ullrich et al [9] showed that the SNR and "contrast-to-noise ratio" (CNR) for T2-weighted images (T2WI) are comparable for both field strengths. However, for diffusion-weighted images (DWI), the SNR and CNR are significantly lower at 1.5T. As DWI is especially important for recognizing csPCa in the peripheral zone (PZ), 3T scanning is preferred. Further investigations are required to understand whether 1.5T has the same diagnostic value as 3T MRI on modern MRI systems for clinical decision making such as the need for biopsy and biopsy yields. Therefore, the use of 3T MRI for prostate imaging is recommended until further investigations shows, that the diagnostic value of 1.5T MRI is sufficient (Table 1). An example of 1.5T versus 3T MRI of the prostate in the same patient is shown in Figure 1.

3. Gradient strength

The SNR and CNR of images are also dependent on the maximum value- and rise-time of the magnetic field gradients. This is especially the case for DWI, where image

Table 1 – Summary of evidence and guidelines for the acquisition of mpMRI of the prostate [36].

	Summary of recommendations	Level of evidence	Grade
Magnetic field strength	3T MRI is preferred to 1.5T MRI	3	B
Gradient strength	Use the strongest gradients possible to increase image quality, especially DWI	3	B
Receiver coils	Use a body phased array and spine coil; an ERC is not necessary	1	A
Patient preparation	Check for MRI-related contraindications	2	B
	Administer antispasmodic agents unless there are contraindications	2	B
	Fasting is not necessary	5	D
	Consider the use of micro-enema prior to a prostate mpMRI examination	3	B
	Use a rectum catheter prior to a prostate mpMRI examination in patients with air in the rectum	5	D
	Ask the patient to refrain from ejaculation during 3 days prior to the MRI examination	2	B
Acquisition protocol	T2WI should always be obtained in the axial plane and at least one other orthogonal plane (sagittal or coronal)	3	B
	The prostate-rectal interface on the sagittal image can be used as a guide for angulation of the coronal plane	3	B
	The axial plane should be positioned perpendicular to the coronal plane	3	B
	DWI is acquired in the axial plane with a small shim box in exactly the same position and same phase encoding direction as the T2WI	3	B
	DWI sequence consists of multiple *b* values, typically b50–100, b400-500, b800 and a high *b* value* of at least b1400s/mm^2	3	B
	DCE-MRI is acquired in the axial plane, in exactly the same position and phase encoding direction as the T2WI and the DWI	3	B
	DCE-MRI is acquired with a high temporal resolution of $<$15 s	3	B
MRI technologist (MRI radiographer) training	Trained technologists (radiographers) specifically for prostate MRI are highly recommended	5	D

DCE = dynamic contrast enhanced; DWI = diffusion-weighted imaging; ERC = endorectal coil; mpMRI = multiparametric MRI; MRI = magnetic resonance imaging; T2WI = T2-weighted imaging.

* A high *b* value image can also be calculatyed from the DWI-series.

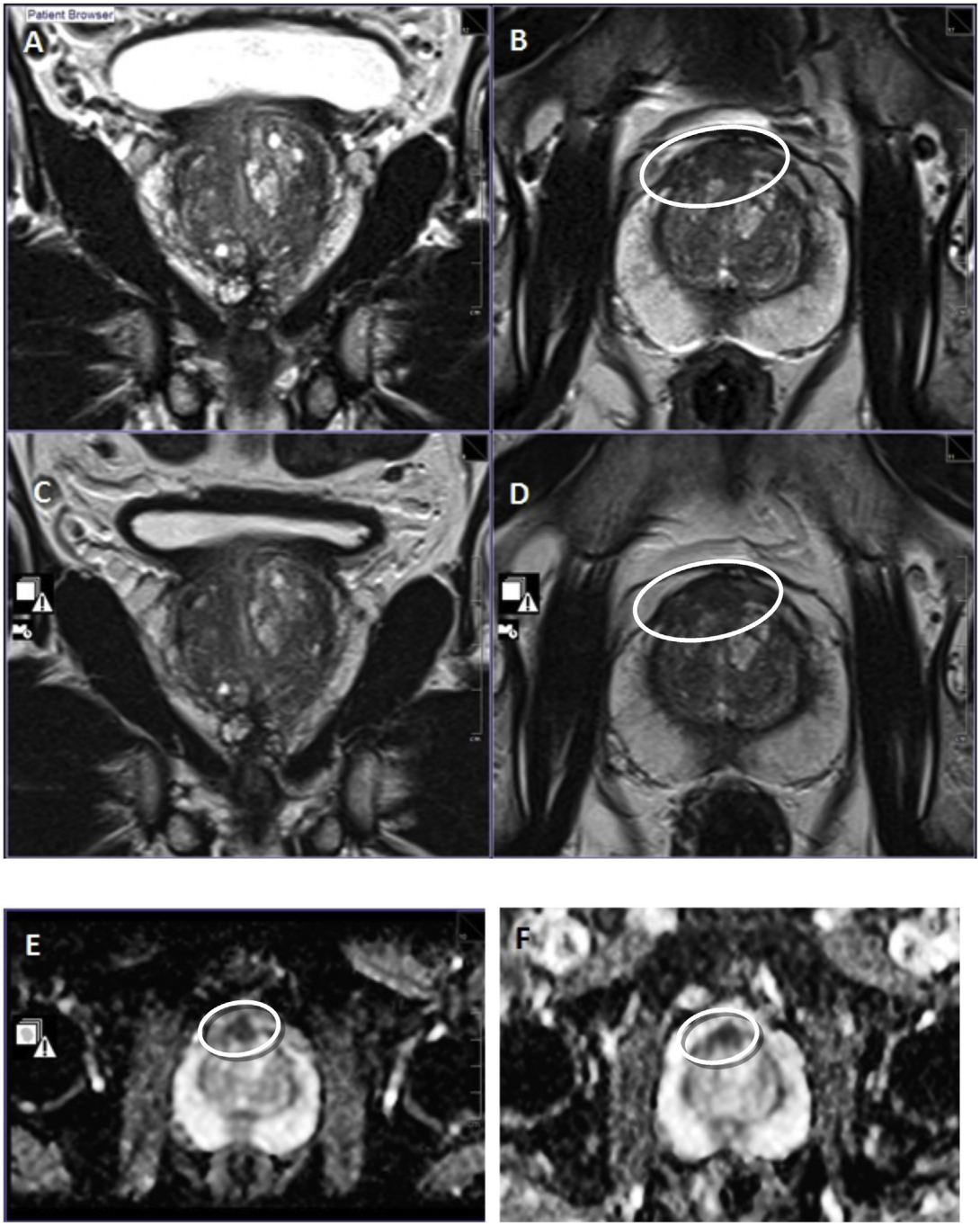

Fig. 1 – Magnetic field strength 3T versus 1.5T MRI: (A,B) 3T axial and coronal T2WI; (C,D) 1.5T axial and coronal T2WI (anterior TZ lesion [circle]); (E) 3T axial ADC map; and (F) 1.5T axial ADC map. Biopsy showed a GG1 (GS 3 + 3) anterior TZ cancer (c.: Professor A. Padhani).
ADC = apparent diffusion coefficient; GG = grade group; GS = Gleason score; MRI = magnetic resonance imaging; T2WI = T2-weighted imaging; TZ = transition zone.

quality highly depends on the gradient strength [10–13]. Stronger gradients allow shorter echo time (TE), enabling a higher SNR and thus better DWI quality [14,15]. However, scanners with higher gradient strength are more expensive, and as a result, many MRI scanners do not fulfill the requirement for short TE times for DWI sequences. As a result, a 3T scanner with low gradient strength will produce lower-quality DWI compared with a 1.5T scanner with high gradient strength. Therefore, strong gradients are preferred over higher magnetic field strength for prostate mpMRI (Table 1).

4. Receiver coils

The most commonly used receiver coil is a body phased array coil in combination with a spine coil. Many centers also employ an additional endorectal coil (ERC). An ERC is a receiver coil in a small balloon that is inserted in the rectum

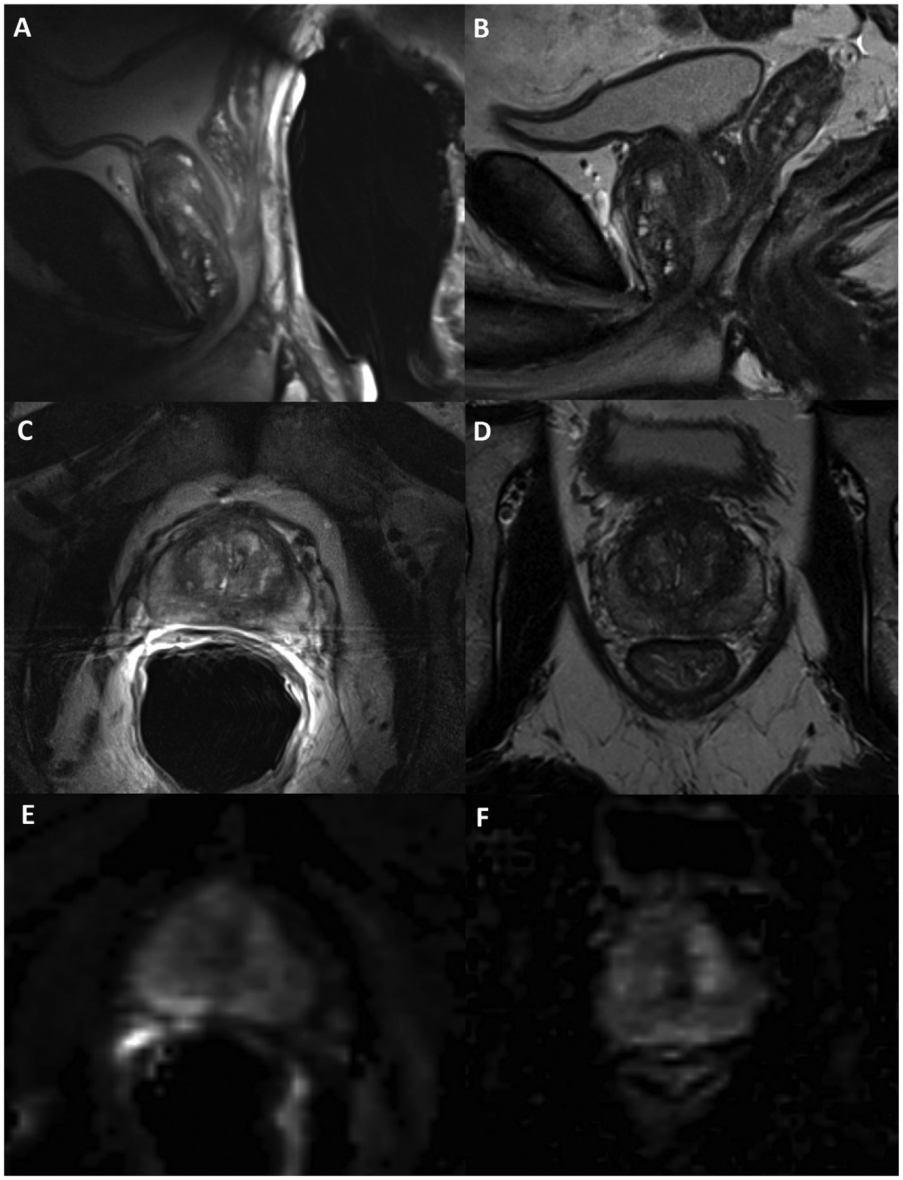

Fig. 2 – ERC versus non-ERC MRI of the prostate. This image shows a patient who underwent 3T MRI (A,C,E) with ERC and (B,D,F) without ERC. (A,B) T2WI sagittal, (C,D) T2WI axial, and (E,F) calculated b1400 images are shown. The images with the use of an ERC show image artifacts at the rectal-prostate interface, and the prostate is noticeably compressed. Whereas the images without an ERC are free from artifacts.
ERC = endorectal coil; MRI = magnetic resonance imaging; T2WI = T2-weighted imaging.

before the MRI examination. The value of an ERC coil for prostate MRI has been studied extensively [16–18]. Its value seems to be for lower field strengths and older MRI machines, where they can improve image quality due to increased SNR. However, major disadvantages of the ERC are artifacts. Research conducted by Husband et al [19] and Sosna et al [20] showed that ERC artifacts are the major causes of decreased image quality.

Recently, there have been multiple improvements in hardware and software, which allow good-quality prostate mpMRI to be obtained without using ERCs [6,21]. Many modern 1.5T MRI scanners do not require an ERC to ensure acceptable image quality. Accordingly, the PI-RADS Committee does not prescribe the use of ERC, stating that reliable, satisfactory results can be obtained with both 1.5T and 3T without the use of an ERC [6]. This position is supported by a systematic review performed by Fusco and colleagues [21] who concluded that new 1.5T and 3T MRI machines can obtain acceptable image quality without the use of an ERC. Figure 2 displays an example of a patient who underwent mpMRI of the prostate both with and without the use of an ERC. Without ERC there are no artifacts and prostate compression. Therefore, mpMRI of the prostate without an ERC is recommended (Table 1).

5. Patient preparation

PI-RADS v2 does not specify patient preparation, mentioning only image quality improvement through the use of antispasmodic agents, preparation enema, a rectum cathe-

Table 2 – Potential contraindications to MRI examination.

Potential contraindications
MRI-unsafe pacemakers, ICDs, neurostimulation systems, cochlear implants, or medication pumps
Metallic foreign bodies, for example, fragments (in the eye), bullets, or shrapnel
Ferromagnetic metallic vascular clips
Metal dental brace/implants
(Severe) claustrophobia
For gadolinium chelate contrast agent:
• Earlier contrast reaction to MRI contrast agent • Poor kidney function (GFR < 30 ml/min/1.73 m^2)

GFR = glomerular filtration rate; ICD = implantable cardioverter defibrillator; MRI = magnetic resonance imaging.

ter, and by refraining from ejaculation for 3 days prior to the MRI [6]. The different patient preparation methods for mpMRI of the prostate are discussed below. A summary of recommendations can be found in Table 1.

5.1. Contraindications

Before undergoing MRI, the patient must be screened for contraindications for MRI to prevent harm. Most important is to check for implants, metal foreign bodies, contrast allergies, and renal function. Shellock and Crues [22] published a review article describing the MR biologic effects and safety guidelines of MR procedures. A list of potential contraindications is listed in Table 2. In case of potential contraindications, this should be discussed with the radiologist. Guidelines concerning contraindications of contrast agents and renal function are described in the ESUR guidelines on contrast media [23].

Postbiopsy hemorrhage is no contraindication for mpMRI of the prostate; a study of Rosenkrantz et al [24] showed that extensive hemorrhage and short delay after biopsy did not negatively impact the accuracy for cs tumor detection using mpMRI. However, the most recent European Association of Urology (EAU) prostate guidelines recommend performing MRI prior to biopsy [25].

5.2. Antispasmodic agents

The administration of an antispasmodic agent such as hyoscine butyl bromide (Buscopan, Boehringer, Ingelheim, Germany) or Glucagon (GlucaGen, Novo Nordisk A/S, Bagsvaerd, Denemarken) can prevent blurring of images by decreasing bowel motility. This has the effect of decreasing peristalsis for a short time (usually around 15–20 min), which is just long enough to acquire the required images [15]. The effect of antispasmodic agents on mpMRI was investigated by Slough et al [26]. The patient group using the antispasmodic agent had significantly higher T2WI quality. Owing to the use of antispasmodic agents, there were less motion artifacts and blurring on the T2WI. However, there was no significant improvement in DWI image quality, or in the degree of DWI distortion or other artifacts. Thus, administration of antispasmodic agents improves image quality of the T2WI and is recommended as patient preparation for prostate MRI. Alternatively, Glucagon may be used when Buscopan is not available/licensed or contraindicated. Contraindications and side effects of antispasmodic agents should be considered. Always consult the medication leaflet before using antispasmodic agents to rule out contraindications and to warn the patient for side effects.

5.3. Fasting

Fasting is another patient preparation method used for abdominal MRI. However, fasting was not mentioned as a preparation method for prostate mpMRI in PI-RADS v2. Evidence for the use of fasting to decrease rectal air or bowel movement is lacking. Fasting is therefore not recommended as a patient preparation method for prostate mpMRI.

5.4. Preparation enema

Caglic and colleagues [27] investigated the effect of rectal distension on prostate mpMR image quality. Rectal distension had a significant negative effect on the quality of both T2WI and DWI. Thus, to optimize image quality, bowel preparation prior to prostate mpMRI should be considered. Lim et al [28] showed that preparatory cleansing enemas did not improve image quality or reduced artifacts in 3T prostate mpMRI. However, van Griethuysen et al [29] investigated the use of a preparatory microenema shortly before the DWI sequence. The microenema consisted of a 5 ml solution (Microlax, McNeil Healthcare, Ireland) that was self-administered by the patient ± 15 min prior to acquisition. Apart from the microenema, no bowel preparation or spasmolytic agents were applied. This significantly reduced both the incidence and the severity of gas-induced artifacts. As gas-induced artifacts especially decrease DWI quality, the use of a microenema prior to a prostate mpMRI examination could be considered where suitable toileting facilities are available.

5.5. Rectum catheter

Air within the rectum can cause susceptibility artifacts that distort DWI. Caglic et al [27] also reported on a strong positive correlation between increased rectal feces and air and DWI distortions/artifacts. Therefore, another option to reduce these artifacts is to decrease the amount of air in the rectum by inserting a rectal catheter prior to the MRI examination and to remove the air with a syringe as suggested by F. Cornud (Paris, France). Figure 3 shows the effect of using such a rectal catheter. Further investigations are required to evaluate whether the use of a rectum catheter could reduce both the incidence and the severity of gas-induced artifacts.

5.6. Refraining from ejaculation

Another preparation mentioned in the PI-RADS recommendations without consensus is the request to refrain

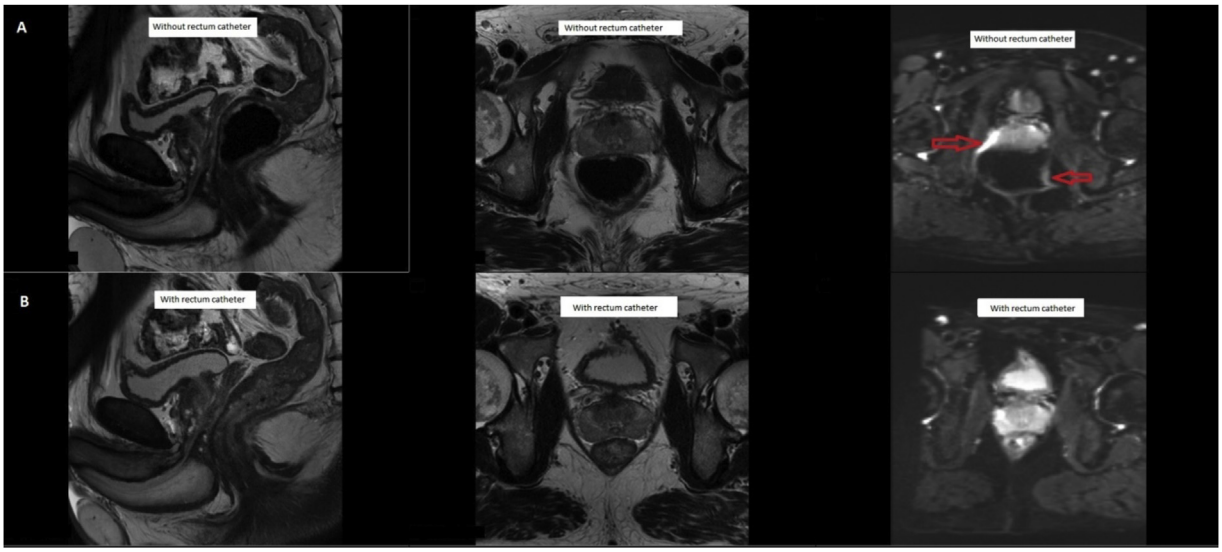

Fig. 3 – Rectum catheter versus no rectum catheter. This image shows a patient who underwent MRI of the prostate (A) without and (B) with the use of a rectum catheter. This demonstrates that, especially in the DWI (right column), susceptibility artifact is present distorting the images where the rectum catheter was not used (arrows), which is considerably improved when the rectum catheter was used.
DWI = diffusion-weighted imaging; MRI = magnetic resonance imaging; T2WI = T2-weighted imaging.

from ejaculation during 3 days prior to the MRI examination. Several articles have examined the influence of ejaculation prior to the MRI examination of the prostate. The main findings were a significant reduction in seminal vesicle (SV) volume after ejaculation and, therefore, decreased diagnostic evaluation of potential SV invasion in patients with known cancers [30–32]. In addition, a significant reduction of prostate apparent diffusion coefficient (ADC) value and significantly decreased T2-value of the PZ have been reported [31,32]. Concluding from these articles, it is reasonable to request that patients refrain from ejaculation for 3 days prior to the MRI examination.

6. Acquisition protocol

According to the PI-RADS v2.1 recommendations, the minimal protocol consists of a combination of high-resolution T2WI in at least two planes, always including an axial plane, and two functional MRI techniques: axial DWI and dynamic contrast enhanced (DCE) MRI [7]. To distinguish the position of a lesion on mpMRI of the prostate, it is important to use similar voxel, slice thickness, and slice positioning for matching between the different sequences. In addition, this will help determine the exact biopsy location. An overview of setting recommendations is presented in Table 1, and Table 3 presents an overview of the recommended minimal sequence parameters for 3T and 1.5T MRI scanners.

6.1. T2-weighted imaging

T2WI shows the prostate's anatomy and is used for the detection, localization, and staging of PCa. In the PZ, PCa can be recognized as a round or ill-defined lesion with low signal intensity on a background of high signal intensity of the normal PZ. Transition zone (TZ) PCa can be more difficult to recognize because low signal intensities of benign prostate hyperplasia can mimic PCa. High-quality T2WI is very important to classify TZ lesions, to evaluate extraprostatic extension, and for planning of fusion biopsies.

T2WI should always be obtained in the axial plane and at least one orthogonal plane (sagittal or coronal), and should include the whole prostate, irrespective of its size and shape, and a minimum of two-thirds of the SV. Angulation of the coronal and axial plane is crucial (although straight axial planes may be more helpful for fusion biopsy planning). For the coronal plane, the prostate-rectal interface on the sagittal image can be used as a guide. When the scan box is parallel to this line, the prostate is "heart shaped" on the coronal plane (Figure 4). This angulation enables optimal visualization of the tumor extension to the SV and comparison of whole-mount section radical prostatectomy slices with (axial) T2WI. The axial plane should be positioned orthogonal to the rectum, that is, perpendicular to the coronal plane [5].

To prevent mismatch between the T2WI axial plane and DWI axial plane, it is important to have a homogenous magnetic field in the prostate itself. To achieve this and to minimize influence of air or bowel movement, a small shim box is applied around the prostate (Figure 5).

The phase encoding direction is an important parameter for the T2WI sequence. A phase encoding direction from left to right is used in the coronal and axial planes to prevent overprojection of motion artifacts from the bowel into the prostate.

Table 3 – Minimal requirements for 3T and 1.5T mpMRI of the prostate.

Sequence	T2 TSE sagittal	T2 TSE coronal	T2 TSE axial	EPI DWI axial	DCE axial
Requirements for 3 T mpMRI of the prostate					
TR (ms)	5590	5000	5660	3200	3.62
TE (ms)	101	101	104	63	1.27
Flip angle (°)	160	160	160	–	14
Freq FOV (mm; phase FOV)	180	192	192	256	192
Matrix size	320	320	320	128	224
# Slices/thickness(mm)	19/3	15/3	19/3	19/3	26/3
Gap (%)	20	20	20	20	–
Voxel size (mm)	0.6 × 0.6 × 3	0.6 × 0.6 × 3	0.6 × 0.6 × 3	2 × 2 × 3	0.9 × 0.9 × 3
Averages/NEX	2	2	2	b50–3	–
				b400–8	
				b800–12	
Phase enc dir	H ≫ F	R ≫ L	R ≫ L	R ≫ L	R ≫ L
≅BW (Hz/Px)	200	200	200	1502	490
b values (s/mm^2; directions)	–	–	–	b50	–
				b400	
				b 800	
				b 1400 (calc.)	
Measurements	1	1	1	1	45
≅Time	2:31	2:15	2:33	4:50	2:50
Requirements for 1.5 T mpMRI of the prostate					
TR (ms)	6700	6500	6400	3700	4.36
TE (ms)	108	146	146	73	1.76
Flip angle (°)	160	160	160	–	12
Freq FOV (mm; phase FOV)	200	200	200	200	260
Matrix size	320	320	320	100	192
# Slices/thickness (mm)	19 /3.5	15/3.5	19/3	19/3	22/3
Gap (%)	20	20	20	20	–
Voxel size (mm)	0.6 × 0.6 × 3.5	0.6 × 0.6 × 3.5	0.6 × 0.6 × 3	2 × 2 × 3	1.4 × 1.4 × 3
Averages/NEX	2	2	2	b50–4	–
				b400–7	
				b800–18	
Phase enc dir	H ≫ F	R ≫ L	R ≫ L	R ≫ L	R ≫ L
≅BW (Hz/Px)	200	200	200	1428	300
b values (s/mm^2; directions)	–	–	–	b50	–
				b400	
				b800	
				b1400 (calc.)	
Measurements	1	1	1	1	40
≅Time	2:22	3:07	3:26	4:33	3:10

BW = band width; DCE = dynamic contrast enhanced; DWI = diffusion-weighted imaging; EPI = echo-planar imaging; FOV = field of view; mpMRI = multiparametric MRI; MRI = magnetic resonance imaging; NEX = number of excitations; Phase enc dir = phase-encoding direction; PX = pixel; TE = echo time; TR = repetition time; TSE = turbo spin echo.

6.2. *Diffusion-weighted imaging*

DWI is an essential sequence for detection and is a predictor of tumor aggression. It reflects the random motion of water molecules and is a key component of the prostate mpMRI examination [6]. PCa demonstrates high signal intensity on DWI at high *b* values (factor of strength and timing of gradients to generate DWI) and low signal intensity on ADC maps. As mentioned above, DWI is acquired in the axial plane with a small shim box in exactly the same position and same phase encoding direction as the T2WI [5]. A typical DWI sequence consists of multiple *b* values, typically b50–100, b400-500, b800, and a high *b* value of at least b1400 s/mm^2. This high *b* value can be acquired separately, but can also be calculated from the lower *b*-value images with monoexponential fitting of the signal decay curve. For the DWI, the ADC map is always calculated using *b* values $<$1000 s/mm^2. The reason for preferably starting with a b50 instead of a b0 is to prevent shine-through of the vessels, that is, to exclude the vascular signals. High *b*-value images are a valuable diagnostic tool in csPCa detection and crucial for mpMRI interpretation [33]. According to the PI-RADS v2.1 standard, a *b* value of $\geq$1400 s/mm^2 must be used for interpretation provided that SNR is sufficient [7].

The image quality of DWI depends on the SNR and the influence of artifacts. With an increased SNR more detailed images can be acquired. The SNR is affected by the following factors: magnetic field strength, proton density of tissues, voxel volumes, TR, TE, flip angle, number of excitations (NEX; also known as the number of signal averages or acquisitions), receiver bandwidth, and coil type [14]. Increasing the *b* values naturally decreases the SNR monoexponentially. To compensate for signal losses in higher *b* values, it is important to increase the NEX with increasing *b* value; for example, we use three NEX for b50, eight NEX for b400, and twelve NEX for b800 to maintain the SNR. Note that this does not alter ADC value calculations.

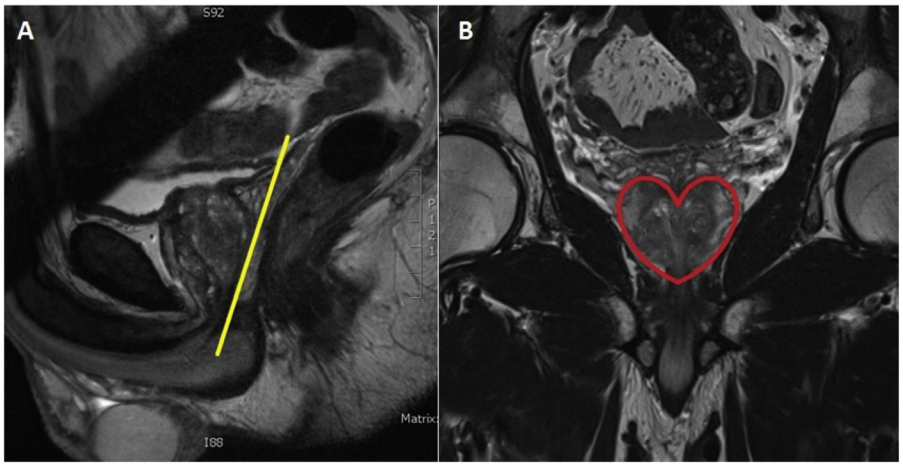

Fig. 4 – Angulation of the coronal plane. (A) Angulation of the coronal plane (yellow line). (B) Heart-shaped coronal view of the prostate with the correct angulation.

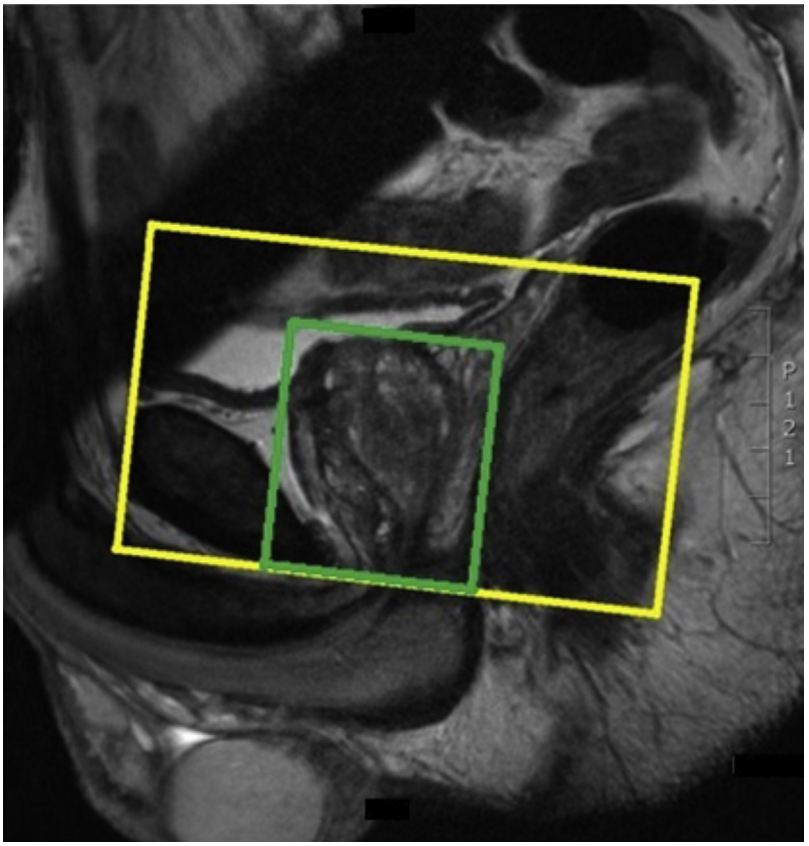

Fig. 5 – Angulation of the axial plane. Angulation of the axial plane (yellow box) and the application of a small shim box around the prostate (green box).

DWI is very sensitive for artifacts that are caused by field inhomogeneities. These inhomogeneities can be caused by a metal hip prosthesis or air in the rectum. Such artifacts can be minimized by using short TE, but they cannot be avoided completely [15]. However, it should be remembered that echo times should not be too short, in order to allow water diffusion to occur prior to the image being acquired. An example of good versus bad high *b*-value DWI image quality can be seen in Figure 6.

6.3. Dynamic contrast enhanced MRI

DCE-MRI during the administration of a gadolinium-containing contrast agent shows tissue vascularity and

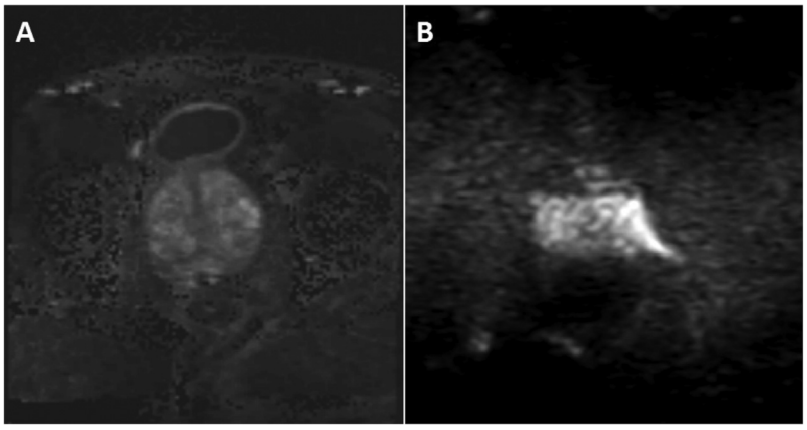

Fig. 6 – DWI image quality. (A) DWI b1400 axial image of the prostate with acceptable image quality. (B) DWI b1400 axial image of the prostate with no acceptable image quality because of a lot of noise and a susceptibility artifact.
DWI = diffusion-weighted imaging.

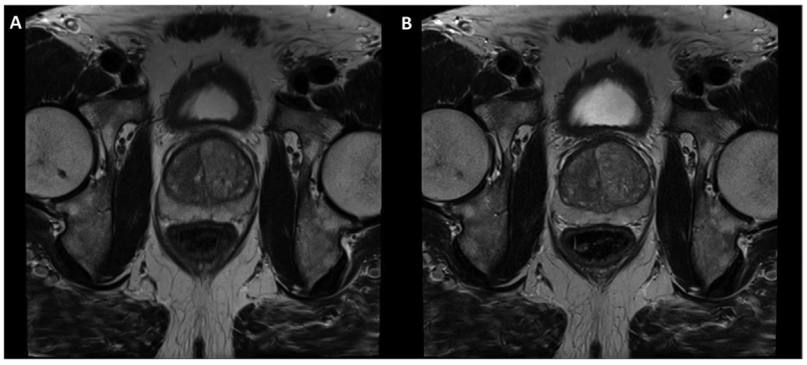

Fig. 7 – Motion artifact. (A) T2W axial image of the prostate with a motion artifact. (B) T2W image of the prostate in the same patient without motion artifacts.
T2W = T2 weighted.

microvessel permeability [5]. Before administrating gadolinium, contrast allergies and renal function should be checked. DCE-MRI is a series of sequential T1-weighted images acquired in the axial plane, in exactly the same position and phase encoding direction as the T2WI and the DWI. A high temporal resolution of $<$15 s is used to show the earlier enhancement of cancer compared with the PZ of the prostate [7]. Contrast enhancement alone is not definitive for csPCa, and absence of early enhancement does not exclude the possibility csPCa. Its value is diminished in TZ assessments. DCE-MRI should be included in all prostate mpMRI examinations so as not to overlook small csPCa [6]. However, the value of mpMRI for detecting csPCa prostate without DCE-MRI is debated [34]. Short MRI protocols without the use of a contrast agent can improve prostate MRI accessibility [35].

7. Artifact prevention

The most common artifacts in mpMRI of the prostate are motion, coil, or patient related. Motion causes blurring of images or ghosting artifacts, and is caused by bowel peristalsis, gland motion, bladder distension, or patient movement. Several approaches can be used to minimize artifacts. One of the most effective ways is good patient preparation. Make the patient as comfortable as possible, a pillow under the knees can help relax the patient and decrease movement of the legs. Clear instructions and communication are the key. Especially tensing of the buttocks and moving of the legs and feet can results in blurred images. As mentioned above, administration of an antispasmodic agent can decrease bowel movements. Decreasing acquisition time per sequence can also prevent motion artifacts. This can be done, for example, with the use of parallel imaging techniques. An example of a motion artifact is shown in Figure 7.

Susceptibility artifacts are another common type of artifacts in prostate MRI that cause distortion of the prostate, especially in DWI. The distortion is caused by local magnetic field inhomogeneities due to rectal air or metal implants (eg, metallic hip prosthesis) [15]. Figure 8 shows an example of distortion caused by rectal air. To

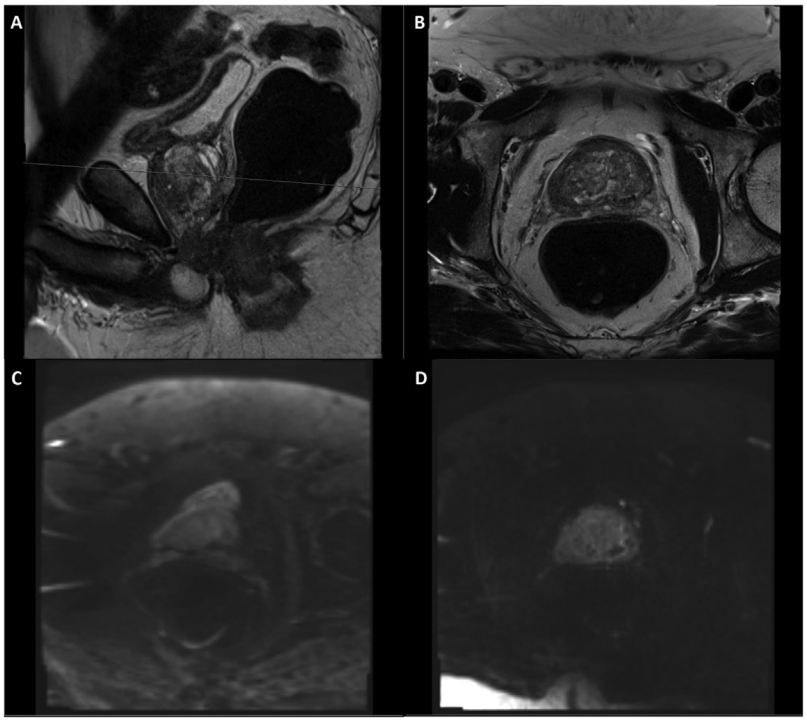

Fig. 8 – Distortion caused by rectal air. A large amount of air in the rectum is visible on the (A) T2 sagittal and (B) T2 axial images. The (C) DWI shows distortion of the prostate caused by rectal air. To decrease the distortion, (D) readout-segmented multishot (RESOLVE) DWI is scanned in the same patient.
DWI = diffusion-weighted imaging.

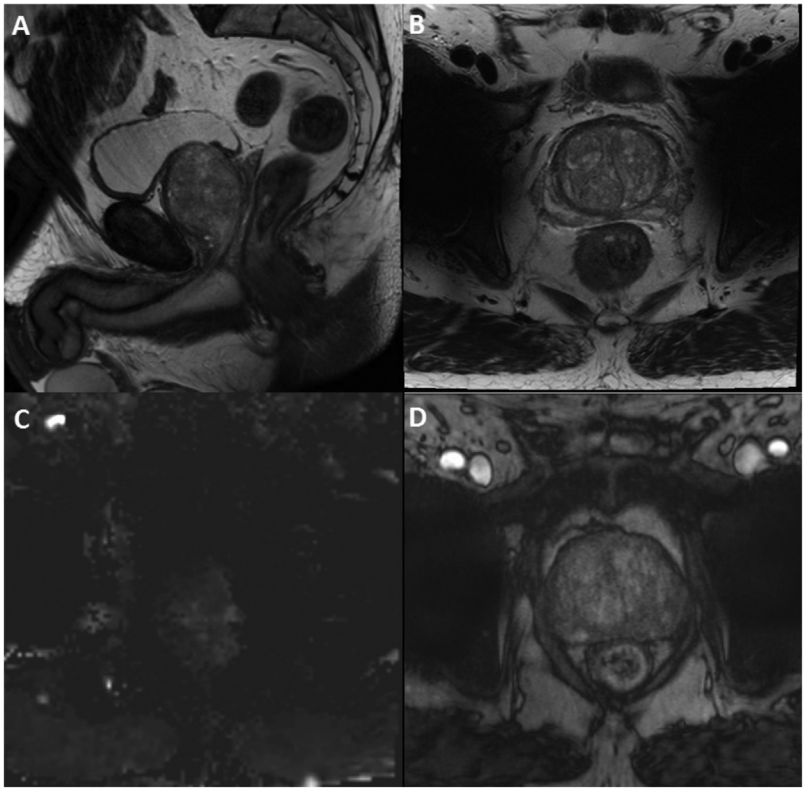

Fig. 9 – Influence of hip prosthesis on image quality. The (A) T2WI sagittal, (B) T2WI axial, and (D) DCE show good image quality to evaluate the prostate. The hip prostheses are displayed as black holes; however, they do not influence the quality of the image in the prostate itself. (C) The DWI is greatly degraded by artifacts and cannot be used for diagnosis.
DCE = dynamic contrast enhanced; DWI = diffusion-weighted imaging; T2WI = T2-weighted imaging.

prevent susceptibility artifacts caused by rectal air, air can be removed with a small rectal catheter (see section 5.5) but also by a small shim box around the prostate. Such a shim box creates a homogenous field in the prostate and prevents susceptibility artifacts.

Susceptibility artifacts caused by metal, for example, hip prosthesis, result in a black hole on T2WI and DWI distortions. Newer image techniques such as readout-segmented DWI might reduce these artifacts. They can also be minimized by using short TE as discussed above, but they cannot be avoided completely [15]. An example of a prostate MR image in a patient with a hip prosthesis is shown in Figure 9. An overview of recommendations for artifact reduction is presented in Table 1.

8. MRI technologists' training

Besides proper patient preparation and technical issues, knowledge and dedication of the performing MRI technologist (MRI radiographer) play a major role in obtaining optimal mpMRI of the prostate. To achieve good image quality, it is important that technologists (radiographers) are properly trained in prostate MRI. Knowledge of anatomy, pathology, and recognizing specific artifacts and technical knowledge will improve the image quality.

9. Conclusions

It is essential that mpMRI scans are PI-RADS v2 compliant and are performed by trained MRI technologists (MRI radiographers) using a standardized protocol consisting of T2WI, DWI, and DCE-MRI. Modern scanners allow obtaining more consistent and high-quality images. Owing to these improvements, an ERC is no longer regarded as necessary, which improves patient comfort and reduces costs. The PI-RADS v2.1 standard gives no specific advice regarding patient preparation. Proper patient preparation and prostate MRI–trained technologists (MRI radiographers) are essential for optimal image quality, and thereby increasing the diagnostic value. It is essential to make patients feel comfortable, with clear instructions and communication before and during the scanning procedure. The use of antispasmodics is recommended, as well as removing air from the rectum where possible. Artifacts can still degrade mpMRI images. By employing modern machines and -techniques, faster image protocols, and optimal patient preparation, these artifacts can be reduced to obtain the best images possible for any given patient. The better the image quality, the easier and better the interpretations by radiologists.

Author contributions: Jelle O. Barentsz had full access to all the data in the study and takes responsibility for the integrity of the data and the accuracy of the data analysis.
Study concept and design: Engels, Israel, Barentsz.
Acquisition of data: Engels, Israel, Barentsz.
Analysis and interpretation of data: Engels, Israel, Padhani, Barentsz.
Drafting of the manuscript: Engels, Israel, Barentsz.
Critical revision of the manuscript for important intellectual content: Engels, Israel, Padhani, Barentsz.
Statistical analysis: None.
Obtaining funding: None.
Administrative, technical, or material support: Barentsz.
Supervision: Barentsz.
Other: None.

Financial disclosures: Jelle O. Barentsz certifies that all conflicts of interest, including specific financial interests and relationships and affiliations relevant to the subject matter or materials discussed in the manuscript (eg, employment/affiliation, grants or funding, consultancies, honoraria, stock ownership or options, expert testimony, royalties, or patents filed, received, or pending), are the following: None.

***Funding/Support and role of the sponsor*:** The production of the video was funded by Soteria Medical. The company did not have any influence on the scientific content of the publication.

***Acknowledgments*:** We would like to thank Tom Scheenen (Radboud University Medical Center, Nijmegen, the Netherlands) and Lynda Drury (Radboud University Medical Center, Nijmegen, the Netherlands) for their contributions to this article. We also like to thank Soteria Medical (Arnhem, NL, USA) for their assistance in producing the video.

Appendix A. Supplementary data

Supplementary material related to this article can be found, in the online version, at doi:https://doi.org/10.1016/j.eururo.2019.09.021.

References

[1] Schoots IG, Roobol MJ, Nieboer D, Bangma CH, Steyerberg EW, Hunink MG. Magnetic resonance imaging-targeted biopsy may enhance the diagnostic accuracy of significant prostate cancer detection compared to standard transrectal ultrasound-guided biopsy: a systematic review and meta-analysis. Eur Urol 2015;68:438–50.
[2] Futterer JJ, Briganti A, De Visschere P, et al. Can clinically significant prostate cancer be detected with multiparametric magnetic resonance imaging? A systematic review of the literature. Eur Urol 2015;68:1045–53.
[3] Rouviere O, Puech P, Renard-Penna R, et al. Use of prostate systematic and targeted biopsy on the basis of multiparametric MRI in biopsy-naive patients (MRI-FIRST): a prospective, multicentre, paired diagnostic study. Lancet Oncol 2019;20:100–9.
[4] van der Leest M, Cornel E, Israël B, et al. Head-to-head comparison of transrectal ultrasound-guided prostate biopsy versus multiparametric prostate resonance imaging with subsequent magnetic resonance-guided biopsy in biopsy-naïve men with elevated prostate-specific antigen: a large prospective multicenter clinical study. Eur Urol 2019;75:570–8.
[5] Barentsz JO, Richenberg J, Clements R, et al. ESUR prostate MR guidelines 2012. Eur Radiol 2012;22:746–57.
[6] Weinreb JC, Barentsz JO, Choyke PL, et al. PI-RADS Prostate Imaging – Reporting and Data System: 2015, version 2. Eur Urol 2016;69:16–40.
[7] Turkbey B, Rosenkrantz AB, Haider MA, et al. Prostate Imaging Reporting and Data System Version 2.1: 2019 update of Prostate

Imaging Reporting and Data System Version 2. Eur Urol 2019;76:340–51.
[8] Mazaheri Y, Vargas HA, Nyman G, Akin O, Hricak H. Image artifacts on prostate diffusion-weighted magnetic resonance imaging: trade-offs at 1.5 Tesla and 3.0 Tesla. Acad Radiol 2013;20:1041–7.
[9] Ullrich T, Quentin M, Oelers C, et al. Magnetic resonance imaging of the prostate at 1.5 versus 3.0T: A prospective comparison study of image quality. Eur J Radiol 2017;90:192–7.
[10] Huang SY, Nummenmaa A, Witzel T, et al. The impact of gradient strength on in vivo diffusion MRI estimates of axon diameter. Neuroimage 2015;106:464–72.
[11] Belli G, Busoni S, Ciccarone A, et al. Quality assurance multicenter comparison of different MR scanners for quantitative diffusion-weighted imaging. J Magn Reson Imaging 2016;43:213–9.
[12] Dietrich O, Biffar A, Baur-Melnyk A, Reiser MF. Technical aspects of MR diffusion imaging of the body. Eur J Radiol 2010;76:314–22.
[13] Bammer R. Basic principles of diffusion-weighted imaging. Eur J Radiol 2003;45:169–84.
[14] Westbrook C, Roth CK, Talbot J. MRI in practice. Oxford, UK: Blackwell Publishing; 2008.
[15] McRobbie DW, Moore EA, Graves MJ, Prince MR. MRI from picture to proton. Cambridge, UK: Cambridge University Press; 2007.
[16] O'Donohoe RL, Dunne RM, Kimbrell V, Tempany CM. Prostate MRI using an external phased array wearable pelvic coil at 3T: comparison with an endorectal coil. Abdom Radiol (NY) 2019;44:1062–9.
[17] Mirak SA, Shakeri S, Bajgiran AM, et al. Three Tesla multiparametric magnetic resonance imaging: comparison of performance with and without endorectal coil for prostate cancer detection, PI-RADS version 2 category and staging with whole mount histopathology correlation. J Urol 2019;201:496–502.
[18] Baur AD, Daqqaq T, Wagner M, et al. T2- and diffusion-weighted magnetic resonance imaging at 3T for the detection of prostate cancer with and without endorectal coil: An intraindividual comparison of image quality and diagnostic performance. Eur J Radiol 2016;85:1075–84.
[19] Husband JE, Padhani AR, MacVicar AD, Revell P. Magnetic resonance imaging of prostate cancer: comparison of image quality using endorectal and pelvic phased array coils. Clin Radiol 1998;53:673–81.
[20] Sosna J, Pedrosa I, Dewolf WC, Mahallati H, Lenkinski RE, Rofsky NM. MR imaging of the prostate at 3 Tesla: comparison of an external phased-array coil to imaging with an endorectal coil at 1.5 Tesla. Acad Radiol 2004;11:857–62.
[21] Fusco R, Sansone M, Granata V, Setola SV, Petrillo A. A systematic review on multiparametric MR imaging in prostate cancer detection. Infect Agent Cancer 2017;12:57.
[22] Shellock FG, Crues JV. MR procedures: biologic effects, safety, and patient care. Radiology 2004;232:635–52.
[23] Contrast Media Safety Committee ESUR. Guidelines on contrast media v10. CMSC. 2018 http://www.esur-cm.org/index.php/en/
[24] Rosenkrantz AB, Mussi TC, Hindman N, et al. Impact of delay after biopsy and post-biopsy haemorrhage on prostate cancer tumor detection using multi-parametric MRI: a multi-reader study. Clin Radiol 2012;67:e83–90.
[25] European Association of Urology. EAU guidelines on prostate cancer. 2019 https://uroweb.org/guideline/prostate-cancer/
[26] Slough RA, Caglic I, Hansen NL, Patterson AJ, Barrett T. Effect of hyoscine butylbromide on prostate multiparametric MRI anatomical and functional image quality. Clin Radiol 2018;73:Error: FPage (216 e9) is higher than LPage (14)!.
[27] Caglic I, Hansen NL, Slough RA, Patterson AJ, Barrett T. Evaluating the effect of rectal distension on prostate multiparametric MRI image quality. Eur J Radiol 2017;90:174–80.
[28] Lim C, Quon J, McInnes M, Shabana WM, El-Khodary M, Schieda N. Does a cleansing enema improve image quality of 3T surface coil multiparametric prostate MRI? J Magn Reson Imaging 2015;42:689–97.
[29] van Griethuysen JJM, Bus EM, Hauptmann M, et al. Gas-induced susceptibility artefacts on diffusion-weighted MRI of the rectum at 1.5T—effect of applying a micro-enema to improve image quality. Eur J Radiol 2018;99:131–7.
[30] Kabakus IM, Borofsky S, Mertan FV, et al. Does abstinence from ejaculation before prostate MRI improve evaluation of the seminal vesicles? AJR Am J Roentgenol 2016;207:1205–9.
[31] Barrett T, Tanner J, Gill AB, Slough RA, Wason J, Gallagher FA. The longitudinal effect of ejaculation on seminal vesicle fluid volume and whole-prostate ADC as measured on prostate MRI. Eur Radiol 2017;27:5236–43.
[32] Shin T, Kaji Y, Shukuya T, Nozaki M, Soh S, Okada H. Significant changes of T2 value in the peripheral zone and seminal vesicles after ejaculation. Eur Radiol 2018;28:1009–15.
[33] Godley KC, Syer TJ, Toms AP, et al. Accuracy of high b-value diffusion-weighted MRI for prostate cancer detection: a meta-analysis. Acta Radiol 2018;59:105–13.
[34] Boesen L, Norgaard N, Logager V, et al. Assessment of the diagnostic accuracy of biparametric magnetic resonance imaging for prostate cancer in biopsy-naive men: the Biparametric MRI for Detection of Prostate Cancer (BIDOC) study. JAMA Netw Open 2018;1:e180219.
[35] van der Leest M, Israel B, Cornel EB, et al. High Diagnostic Performance of Short Magnetic Resonance Imaging Protocols for Prostate Cancer Detection in Biopsy-naive Men: The Next Step in Magnetic Resonance Imaging Accessibility. Eur Urol 2019.
[36] Phillips B, Ball C, Sackett D, et al. Oxford Centre for Evidence-based Medicine—levels of evidence. 2019 https://www.cebm.net/2009/06/oxford-centre-evidence-based-medicine-levels-evidence-march-2009/

EUROPEAN UROLOGY 77 (2020) 469–480

available at www.sciencedirect.com
journal homepage: www.europeanurology.com

European Association of Urology

Surgery in Motion

Multiparametric Magnetic Resonance Imaging for the Detection of Clinically Significant Prostate Cancer: What Urologists Need to Know. Part 2: Interpretation

Bas Israël[a], *Marloes van der Leest*[a], *Michiel Sedelaar*[b], *Anwar R. Padhani*[c], *Patrik Zámecnik*[a], *Jelle O. Barentsz*[a,*]

[a] *Department of Radiology and Nuclear Medicine, Radboud university medical center, Radboud Institute for Health Sciences, Nijmegen, The Netherlands;* [b] *Department of Urology, Radboud university medical center, Radboud Institute for Health Sciences, Nijmegen, The Netherlands;* [c] *Paul Strickland Scanner Centre, Northwood, UK*

Article info

Article history:
Accepted October 21, 2019

Associate Editor: Alexandre Mottrie

Keywords:
Prostate cancer
Magnetic resonance imaging
Multiparametric magnetic resonance imaging
Interpretation prostate imaging reporting and data system version 2
Prostate imaging reporting and data system

Please visit www.europeanurology.com and www.urosource.com to view the accompanying video.

Abstract

Background: There is large variability among radiologists in their detection of clinically significant (cs) prostate cancer (PCa) on multiparametric magnetic resonance imaging (mpMRI).
Objective: To reduce the interpretation variability and achieve optimal accuracy in assessing prostate mpMRI.
Design, setting, and participants: How the interpretation of mpMRI can be optimized is demonstrated here. Whereas part 1 of the "surgery-in-motion" paper focused on acquisition, this paper shows the correlation between (ab)normal prostate anatomical structures and image characteristics on mpMRI, and how standardized interpretation according to Prostate Imaging Reporting and Data System version 2 (PI-RADS v2) should be performed. This will be shown in individual patients.
Surgical procedure: To detect csPCa, three mpMRI "components" are used: "anatomic" T2-weighted imaging, "cellular-density" diffusion-weighted imaging, and "vascularity" dynamic contrast-enhanced MRI.
Measurements: Based on PI-RADS v2, the accompanying video shows how mpMRI interpretation is performed. Finally, the role of mpMRI in detecting csPCa is briefly discussed and the main features of the recently introduced PI-RADS v2.1 are evaluated.
Results and limitations: With PI-RADS v2, it is possible to quantify normal and abnormal anatomical structures within the prostate based on its imaging features of the three mpMRI "components." With this knowledge, a more objective evaluation of the presence of a csPCa can be performed. However, there still remains quite some space to reduce interobserver variability.
Conclusions: For understanding the interpretation of mpMRI according to PI-RADS v2, knowledge of the correlation between imaging and (ab)normal anatomical structures on the three mpMRI components is needed.
Patient summary: This second surgery-in-motion contribution shows what structures can be recognized on prostate magnetic resonance imaging (MRI). How a radiologist performs his reading according to the so-called Prostate Imaging Reporting and Data System criteria is shown here. The main features of these criteria are summarized, and the role of prostate MRI in detecting clinically significant prostate cancer is discussed briefly.

* Corresponding author. Department of Radiology and Nuclear Medicine, Radboud University Nijmegen Medical Center, P.O. Box 9101, Nijmegen, The Netherlands. Tel. +31243619196, +31625015262, Fax: +31243540866.
E-mail address: jelle.barentsz@radboudumc.nl (J.O. Barentsz).

https://doi.org/10.1016/j.eururo.2019.10.024

1. Prostate multiparametric magnetic resonance imaging

Magnetic resonance imaging (MRI) is a noninvasive imaging technique that uses the interaction between radiofrequency pulses, a strong magnetic field, and body tissue, to obtain images of planes inside the body. Compared with other imaging modalities, such as ultrasound and computed tomography (CT) scanning, MRI is superior in soft tissue imaging [1]. Unlike x-rays and CT scans, MRI uses no radiation. The recommended technique of MRI in prostate cancer (PCa) is multiparametric-MRI (mpMRI), which includes high-resolution T2-weighted (T2W) images to depict prostate anatomy and two functional MRI techniques, including diffusion-weighted imaging (DWI) to display cell density and dynamic contrast-enhanced MRI (DCE-MRI) that shows vascularity.

Clinical indications for mpMRI of the prostate include detection and localization of primary PCa for guidance of MRI-directed biopsy (MRDB), local staging, assessment of suspected PCa recurrence, active surveillance, and local treatment (eg, surgery, radiation therapy, and focal therapy) [2–7].

1.1. T2-weighted imaging

T2W imaging (T2WI) shows anatomic-morphologic features of the prostate and morphologic-pathologic structures. T2W images are acquired preferably in three perpendicular planes (axial, coronal, and sagittal). These show the anatomic prostate zonal anatomy and the relation of the prostate to its surrounding structures. T2WI is ideal to differentiate between the high-signal peripheral zone (PZ), the heterogeneous mixed-signal transition zone (TZ), and the low-signal central zone (CZ). The high-signal of the PZ is caused by cystic degeneration with high fluid content and is usually surrounded by a thin hypointense rim that represents the pseudocapsule. This rim is an important landmark for tumor staging [8]. The TZ usually has a heterogeneous mixed signal due to the various stages of the benign prostatic hypertrophy (BPH) nodules (Fig. 1). BPH can be degenerative or can show cellular hypertrophy. On T2WI, this BPH-changed TZ is often referred to as "organized chaos." The CZ has more dense fibrous tissue and, therefore, a low signal on T2WI.

On T2WI, lesions can be anatomically localized, and their shape, form, and size are assessed. Zonal distinction of the prostate is important as approximately 70–75% of PCa cases arise from the PZ, and the Prostate Imaging Reporting and Data System (PI-RADS) assessment is zonal based [9–11]. The high-signal PZ may be disrupted as an area of a lower signal due to the presence of PCa. However, PCa can also present as isosignal areas or nonfocal mildly hypointense abnormalities. Low-grade PCa or nonmalignant conditions, such as scar tissue, hemorrhage, atrophy, postradiation changes, and (granulomatous) prostatitis, frequently have a low signal intensity; thus, based on its signal on T2WI, it cannot be differentiated from clinically significant (cs) PCa [12,13]. To some extent, using anatomic-morphologic structures for the differentiation of csPCa from low-grade PCa and benign pathology is possible [7]. A focal, round, or irregular structure is more likely to be csPCa,

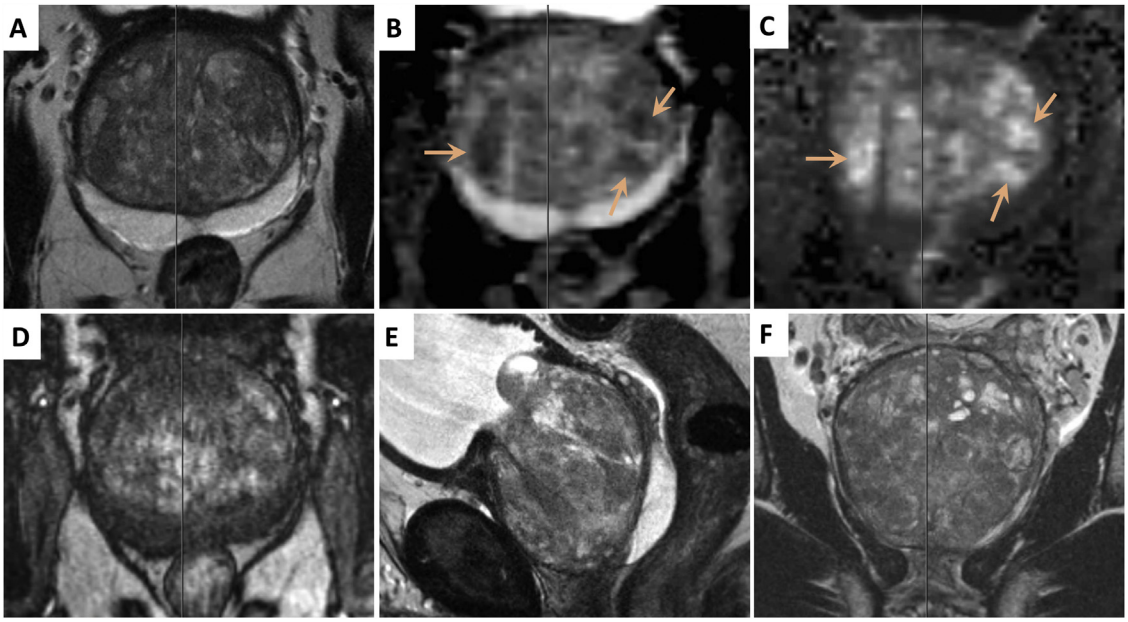

Fig. 1 – PI-RADS 1 (BPH) assessment of a patient aged 56 yr, having cT0, PSA 13, 219 cc, PSAd 0.06. (A) Axial, (E) sagittal, and (F) coronal T2W images show well-circumscribed nodules in the TZ, which are surrounded by a low-signal rim. Normal (bright) PZ. Some nodules show restricted diffusion: "dark" on (B) axial ADC map and" white" on (C) *b* 1400 (arrows). For BPH, this is normal. (D) Axial DCE images show minimal "pop-corn" enhancement that is typical for BPH nodules. This is scored as "–". Thus the score T2W/DWI/DCE is 1/1/–, with PI-RADS v2.1 category 1 (BPH). TRUS biopsy revealed no abnormalities. ADC = apparent diffusion coefficient; BPH = benign prostatic hypertrophy; DCE = dynamic contrast enhanced; DWI = diffusion-weighted imaging; PI-RADS = Prostate Imaging Reporting and Data System; PSA = prostate-specific antigen; PSAd = PSA density; PZ = peripheral zone; TRUS = transrectal ultrasound; T2W = T2 weighted; TZ = transition zone.

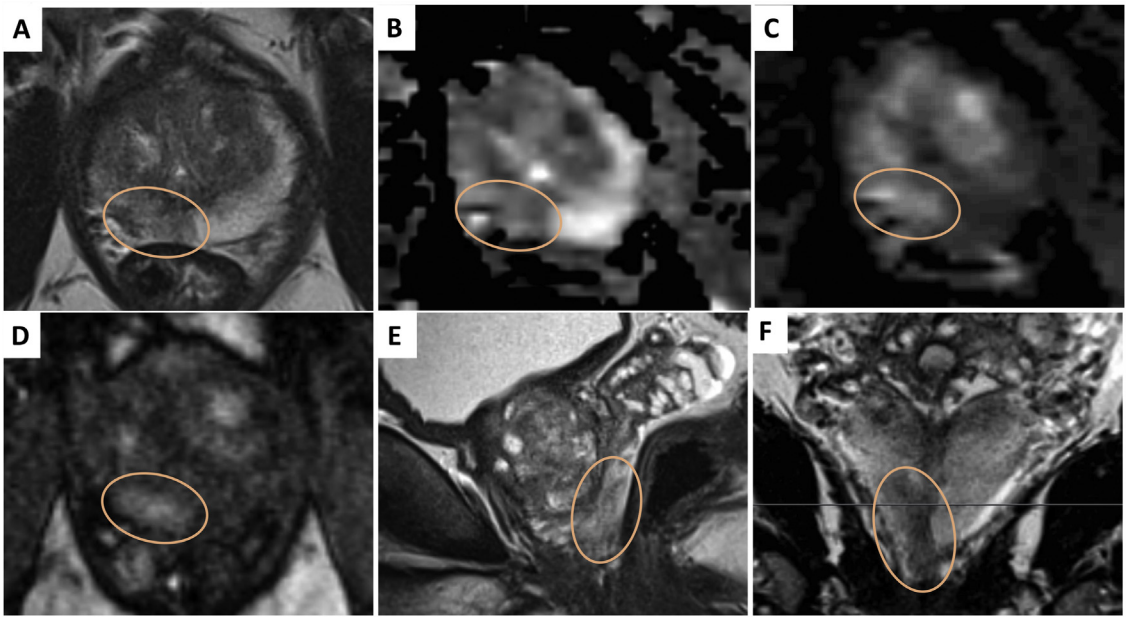

Fig. 2 – PI-RADS 2 (prostatitis) assessment of a patient aged 61 yr, having cT0, PSA 5.1, 63 cc, PSAd 0.08. (A) Axial, (E) sagittal, and (F) coronal T2W images show linear and wedge-shaped mild hypointensities of the right PZ (orange circle). (B) Indistinct diffuse minimal hypointense signal on ADC map and (C) no "high signal" on *b* 1400 (orange circles). (D) DCE images show early enhancement (bright signal) of the right PZ (orange circle). Score: T2W/DWI/DCE: 2/2/+. This results in PI-RADS v2.1 category 2 (prostatitis). TRUS biopsy showed chronic inflammation. ADC = apparent diffusion coefficient; DCE = dynamic contrast enhanced; DWI = diffusion-weighted imaging; PI-RADS = Prostate Imaging Reporting and Data System; PSA = prostate-specific antigen; PSAd = PSA density; PZ = peripheral zone; TRUS = transrectal ultrasound; T2W = T2 weighted; TZ = transition zone.

whereas prostatitis is marked by a wedge-shaped and more diffuse appearance (Fig. 2) [14,15]. The diagnosis of csPCa in the TZ imposes a greater challenge than in the PZ. Features indicative of TZ cancers are ill-defined margins; focal homogeneous T2 intermediate-low signal ("erased charcoal drawing sign"); noncircumscribed, lenticular, or fusiform shape; and invasion of the surrounding structures ("disruption of organized chaos"; Fig. 3) [7]. To determine whether an abnormal region is suspicious for csPCa, T2WI should be used in conjunction with the other two functional imaging techniques.

1.2. *Diffusion-weighted imaging*

On T2WI, differentiation of csPCa from low-grade PCa, fibrous tissue, inflammation, postbiopsy hematoma, and glandular BPH nodules is difficult. Thus, DWI is needed for further evaluation of tissue characteristics. DWI is the most important functional imaging technique because it corresponds to histopathologic findings [16–19]. DWI shows the velocity (diffusion) of intracellular water. In dense cellular tissue, this velocity is reduced; therefore, diffusion is restricted. This is visible as a low signal (black) on the DWI-derived velocity map: the apparent diffusion coefficient (ADC) map [20,21]. Low cell density has a high signal (white) on the ADC map. Another DWI-derived image that is used is the high *b*-value ($\geq$1400 s/mm^2) image. On these images, high cell density has a high signal (white) and low cell density is dark [22,23]. On DWI, the normal PZ has a high signal (white) due to its high content of fluid-filled glandular structures and high velocity of water molecules [24,25]. Clinically significant PCa replaces healthy glandular tissue and has high cell density; therefore, it is visible as a low signal on the ADC map (restricted diffusion). There is an inverse relationship between ADC value and Gleason score (GS), that is, decreasing ADC values (low signal) correlate significantly with increasing GSs [26–28]. However, in the TZ, BPH can also show restricted diffusion; hence, DWI is more accurate for csPCa detection in the PZ than in the TZ [29]. A focal lesion is more likely to be csPCa than a more diffuse lesion (eg, prostatitis). Finally, DWI is highly susceptible to artifacts. Bowel peristalsis, total hip prosthesis, or gas in the rectum (susceptibility artifacts) can limit DWI quality.

1.3. *DCE and T1-weighted imaging*

DCE-MR images are T1-weighted (T1W) images that show tissue enhancement (vascularization) after bolus injection of an MR contrast agent. Owing to tumor angiogenesis and higher vessel permeability, both low-grade PCa and csPCa, cellular-BPH, and inflammation show earlier and more pronounced enhancement compared with other prostate tissue [30,31]. Thus, accurate differentiation of benign prostate structures such as (highly vascularized) prostatitis in the PZ or (highly perfused) cellular BPH in the TZ from csPCa is limited. DCE-MRI is of essential value for the detection of local recurrences (eg, postradiotherapy or after radical prostatectomy) [4,32]. In untreated patients, DCE-MRI helps identify prostatitis and is of value in "equivocal"

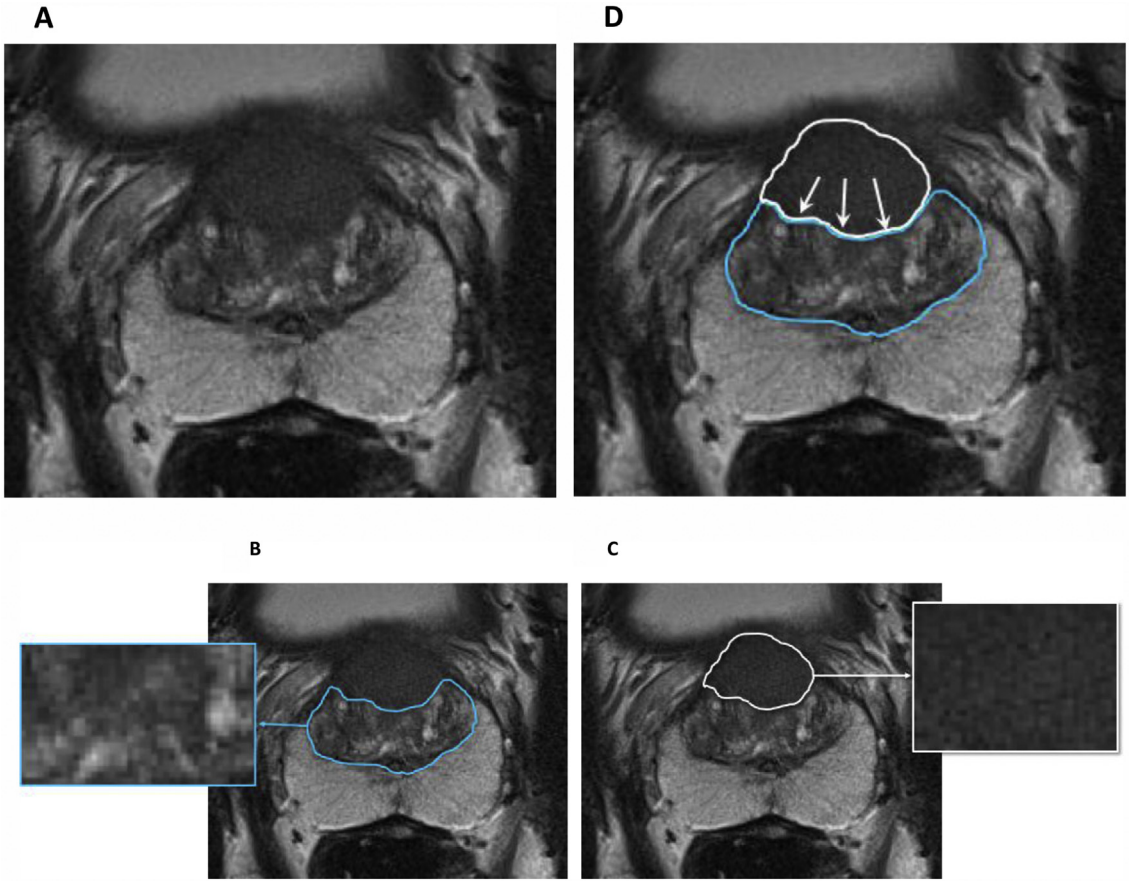

Fig. 3 – PI-RADS 5 TZ lesion: disruption of BPH ("organized chaos") by ISUP grade 3 PCa ("erased charcoal"). (A) Axial T2W image through midprostate shows a normal bright PZ. (B) BPH in the TZ is visible as "organized chaos" (blue area, magnified in box). (C) Ventral to the BPH a homogeneous intermediate signal "erased charcoal" area is visible (white, magnified in box). (D). This area (TZ PI-RADS 5 lesion; ISUP grade 3 on targeted biopsy) shows "disruption of organized chaos" (arrows). BPH = benign prostatic hypertrophy; ISUP = International Society of Urological Pathology PCa = prostate cancer; PI-RADS = Prostate Imaging Reporting and Data System; PZ = peripheral zone; T2W = T2 weighted; TZ = transition zone.

findings in the PZ. Unenhanced (precontrast) T1W imaging is the only technique to identify postbiopsy hemorrhage by its high T1W signal [33].

2. MRI interpretation

2.1. *PI-RADS version 2*

In 2012, the prostate MR working group of the European Society of Urogenital Radiology (ESUR) initiated a guideline (PI-RADS v1) to standardize mpMRI acquisition, and interpretation and reporting of mpMRI scans [14]. A second version of PI-RADS (v2) was developed by a joint steering committee of the ESUR, the American College of Radiology, and the AdMeTech Foundation [7]. More recently, an updated version (v2.1) was published [34]. This updated version aimed to further simplify the assessment and reporting, as well as to reduce interpretation variability of prostate mpMRI.

PI-RADS is a risk assessment tool based on a standardized evaluation method to predict the likelihood that csPCa is present. Each detected lesion is scored separately using a standardized description for the three individual MRI techniques: T2WI, DWI, and DCE-MRI. Thereafter, they are combined to give an overall assessment category score, from 1 (csPCa is highly unlikely to be present) to 5 (csPCa is highly likely to be present; Table 1). PI-RADS v2.1

Table 1 – PI-RADS v2 assessment categories and risk of (cs)PCa.

PI-RADS v2 categories	Risk of csPCa	% PCa [36,40,42,43,46,48,59,60]	% csPCa (ISUP grade ≥2)
1–2	(Very) low	13–24	3–12
3	Equivocal	34–50	4–27
4	High	60–77	32–60
5	Very high	91–97	67–83

csPCa = clinically significant prostate cancer; ISUP = International Society of Urological Pathologt PCa = prostate cancer; PI-RADS v2 = Prostate Imaging Reporting and Data System version 2.

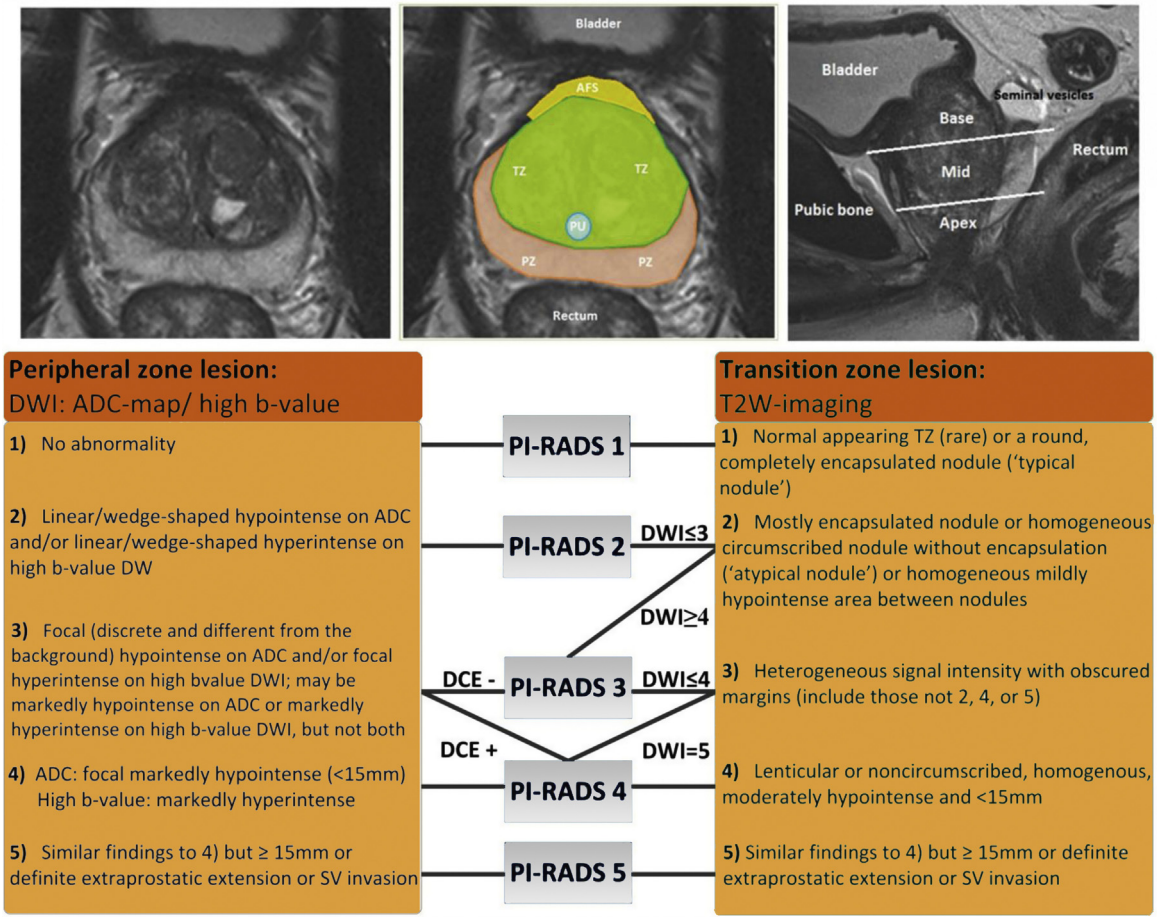

Fig. 4 – Prostate zonal anatomy and PI-RADS v2.1 assessment. ADC = apparent diffusion coefficient; AFS = anterior fibromuscular stroma; DCE = dynamic contrast enhanced; DWI = diffusion-weighted imaging; PI-RADS = Prostate Imaging Reporting and Data System; SV = seminal vesicle; PU = prostatic urethra; PZ = peripheral zone; T2W = T2 weighted; TZ = transition zone.

emphasizes the dominant role of DWI as the parameter for any suspicious lesion(s) found in the PZ and T2WI, in combination with DWI in TZ lesions (Fig. 4). DCE-MRI scores are a binary assessment, and its role is limited to upgrading DCE-MRI–positive lesion(s) in the PZ from PI-RADS category 3 to 4. A more precise division of prostate sectors was proposed [15,34].

2.2. How to score lesions (video)

For optimal reading, a dedicated workstation should be used that shows all images in one view: triplanar T2WI, axial ADC map, axial high *b*-value DWI, and axial (cine-loop) DCE-MRI. In addition, a cross-correlation tool, such as a "cross-hair" should be used, which enables a specific area in one view to be evaluated on all images.

First, image quality must be assessed. If the quality is insufficient, either this should be reported (as PI-RADS category X) or the patient must undergo additional imaging to obtain better images. Feedback should be given to the technologist and corrective measures should be implemented. Then the maximal prostate dimensions on T2WI are measured in three perpendicular planes (anterior-posterior [AP], left-right [LR], and cranial-caudal [CC]), and prostate volume ($AP \times LR \times CC \times 0.52$) and prostate-specific antigen (PSA) density (PSAd = PSA divided by prostate volume) are calculated. After appropriate adjustments of the contrast and brightness (so-called "window" and "center") of the images, suspicious lesions are looked for on all T2WI planes.

Before any lesion is scored (characterized), it needs to be detected. PI-RADS is agnostic about lesion detection method. We suggest that T2WI, high *b*-value DWI, and early post–contrast enhancement images be evaluated initially for any lesion(s) that could represent csPCa, based on morphologic findings, signal characteristics, or enhancement patterns. These features need not be confined to those described for scoring purposes; lesions or regions that could be abnormal need to be detected prior to PI-RADS v2.1 characterization. However, special attention should be placed on TZ lesions that show "erased charcoal" or "disruption of organized chaos," and PZ lesions that are "black" on the ADC-map and "white" on the high *b*-value DWI. These should be evaluated for a likelihood of csPCa using PI-RADS.

Location assessment of a lesion in either the PZ or the TZ/CZ is of utmost importance, as these zones have a different

"dominant" sequence according to PI-RADS. If a lesion is identified on T2WI, its signal intensity, size, and appearance should be determined on the ADC map and the high *b*-value ($b \geq 1400 s/mm^2$) DWI.

A focal mass in the PZ with a low signal on the ADC map and a high signal on the high *b*-value DWI has a PI-RADS 4 or 5 assessment, with the distinction being determined by size (cutoff: 15 mm) or extracapsular extension (Fig. 5–7). If a TZ has an "erased charcoal" appearance and/or there is "disruption of organized chaos" on T2WI, or if an anterior TZ lesion has a "lenticular shape," then the PI-RADS assessment is also 4 or 5 (Fig. 6). Usually, a csPCa located in the TZ also has a low signal on the ADC map and a high signal on high *b*-value DWI. However, cellular BPH may have

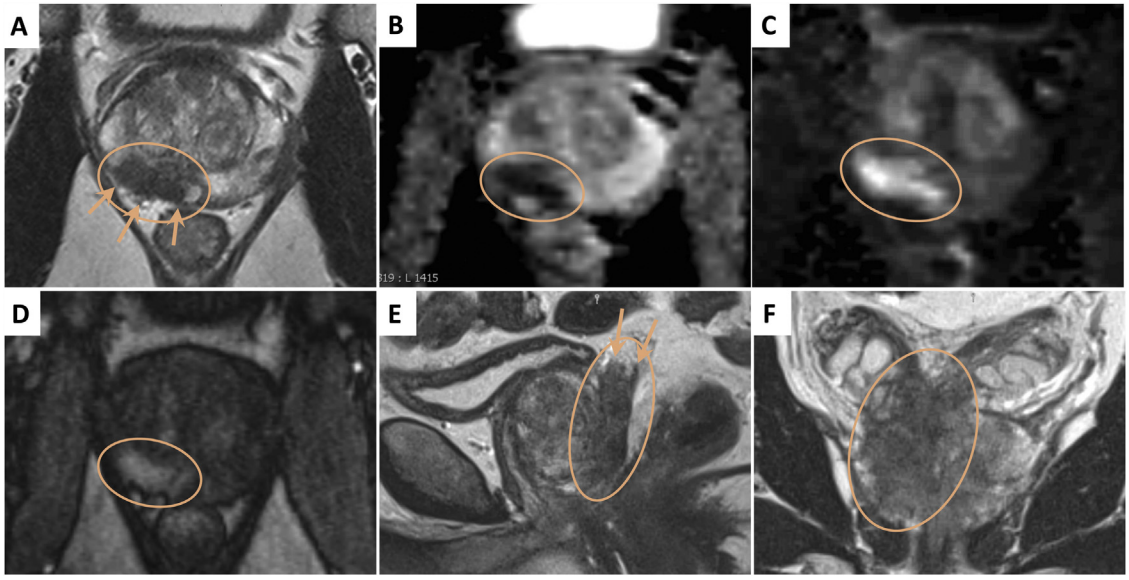

Fig. 5 – PI-RADS 5 assessment of a patient aged 74 yr, with cT2 on the right side, PSA 7.1, 64 cc, PSAd 0.11). (A) Axial, (E) sagittal, and (F) coronal T2W images show low-signal lesion midprostate, PZ, 6–9 o'clock (orange circles). ADC shows a (B) focal "black" area with a low ADC value (600) and (C) focal "white" area on *b* 1400. (D) On DCE image, this lesion shows early focal enhancement. (A) axial T2W image shows extracapsular extension (arrows) MRI stage T3a. (E) Sagittal T2W image shows seminal vesicle infiltration (arrows) MRI stage T3b. Transperineal fusion biopsy showed PCa ISUP grade 3. Score: T2W/DWI/DCE: 5/5/+. This results in PI-RADS v2.1 category 5 (high risk for csPCa). ADC = apparent diffusion coefficient; csPCa = clinically significant prostate cancer; DCE = dynamic contrast enhanced; DWI = diffusion-weighted imaging; ISUP = International Society of Urological Pathology; MRI = magnetic resonance imaging; PCa = prostate cancer; PI-RADS = Prostate Imaging Reporting and Data System; PSA = prostate-specific antigen; PSAd = PSA density; PZ = peripheral zone; T2W = T2 weighted.

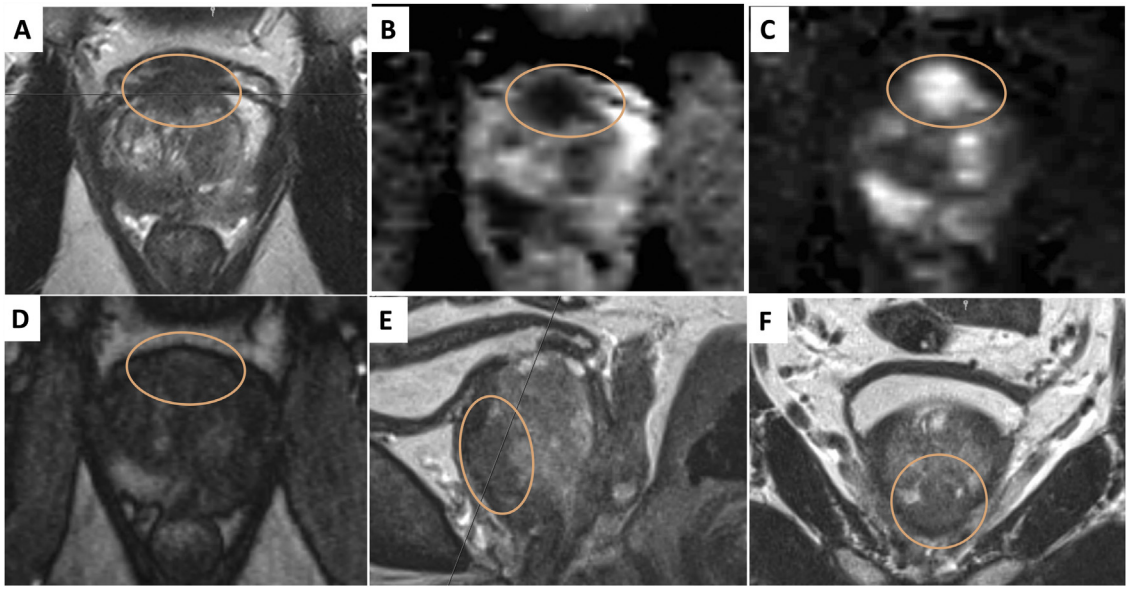

Fig. 6 – Same patient as in Fig. 5, lesion #2: PI-RADS 5. (A) Axial, (E) sagittal, and (F) coronal T2W images show a low-signal lesion apex to midprostate, TZ, 11–1 o'clock (orange circles), with diameter >15 mm. (B) ADC shows a focal "black" area with a low ADC, which is (C) a focal "white" area on *b* 1400. (D) DCE image does not show early focal enhancement. Score: T2W/DWI/DCE: 5/5/–. This results in PI-RADS v2.1 category 5. Transperineal fusion biopsy showed PCa ISUP grade 2. ADC = apparent diffusion coefficient; DCE = dynamic contrast enhanced; DWI = diffusion-weighted imaging; ISUP = International Society of Urological Pathology; PCa = prostate cancer; PI-RADS = Prostate Imaging Reporting and Data System; T2W = T2 weighted; TZ = transition zone.

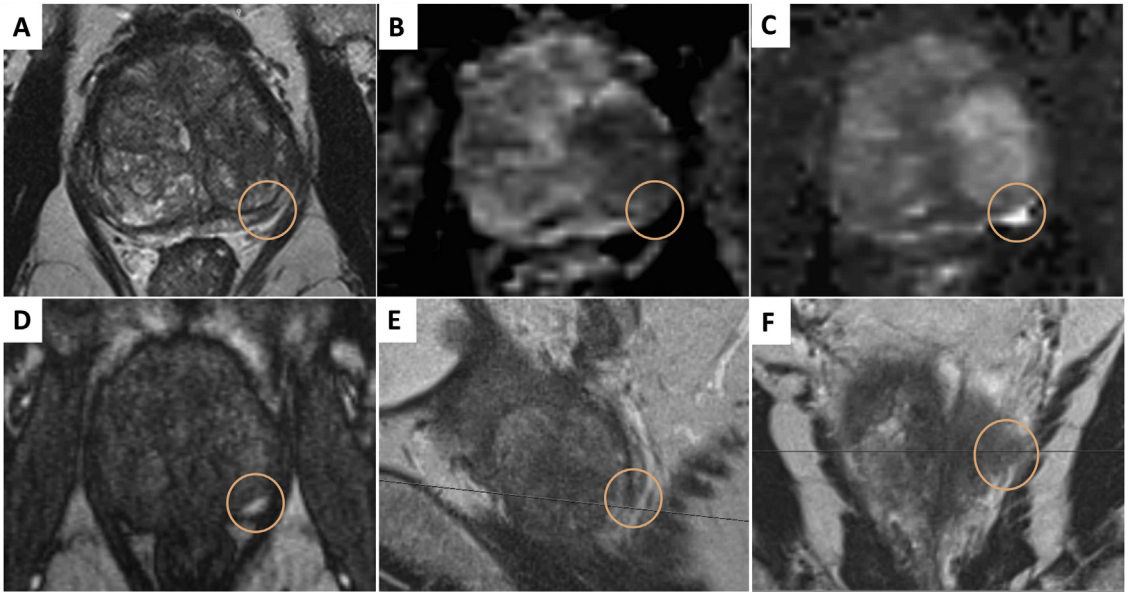

Fig. 7 – PI-RADS 4 assessment of a patient aged 70 yr, with cT0, PSA 9.8, 115 cc, PSAd 0.08. (A) Axial, (E) sagittal, and (F) coronal T2W images show a $3 \times 5 \times 8$ mm^3 small focal low-signal-intensity lesion at midprostate, PZ, 4–5 o'clock (lesion is within orange circles). DWI shows (B) no focal low signal on ADC map and (C) a focal high signal intensity on *b* 1400. (D) The DCE-MRI shows marked early focal enhancement. Score: T2W/DWI/DCE: 4/3/+. This results in PI-RADS v2.1 category 4 (at risk for csPCa). MR-TRUS fusion biopsy showed PCa ISUP grade 4. ADC = apparent diffusion coefficient; csPCa = clinically significant prostate cancer; DCE = dynamic contrast enhanced; DWI = diffusion-weighted imaging; ISUP = International Society of Urological Pathology; MRI = magnetic resonance imaging; PCa = prostate cancer; PI-RADS = Prostate Imaging Reporting and Data System; PSA = prostate-specific antigen; PSAd = PSA density; PZ = peripheral zone; TRUS = transrectal ultrasound; T2W = T2 weighted.

similar appearance on DWI, and the corresponding T2WI should therefore be determinant. In the TZ, partially encapsulated or circumscribed, encapsulated nodules (T2WI score of 2) with clearly restricted diffusion (DWI score 4 or 5) receive a final score of PI-RADS 3. TZ lesions with a T2WI score of 3 and a DWI score of 5 (ie, >1.5 cm) are assessed as PI-RADS 4 lesions (Fig. 4).

Finally, the DCE-MRI sequence must be evaluated to see whether early enhancement in the PZ matches with a wedge-shaped or diffuse intermediate signal ADC lesion (ie, prostatitis), or a detected/undetected focal lesion. If a lesion in the PZ is scored 3 on DWI but shows early focal enhancement, the final PI-RADS assessment is 4 (Fig. 7).

Up to four lesions are assessed. The lesion with the highest PI-RADS score is called the "index lesion." Its location, size, lowest ADC value, and risk of extraprostatic extension (either extracapsular extension or seminal vesicle infiltration) are reported.

2.3. Clinical parameters

Although the PI-RADS v2.1 score is assigned solely on the mpMRI assessments, clinical (risk) factors should also be considered, as these are of importance for decision making. The following clinical information should be available to radiologists at the time of reporting: digital rectal examination findings, family history, PSA history and most recent PSA level, previous biopsy status (in case of a prior biopsy, date and histopathologic findings), prior prostate and/or pelvic surgery, and medication affecting the PSA level.

The MRI-derived PSAd is important to know during the interpretation of the images. If the PSAd is above a certain cutoff level (eg, ≥0.15 ng/ml/ml), the radiologist should be very cautious not to miss a csPCa and should seek an explanation for the elevated PSAd, for example, prostatitis or csPCa [35]. It is important to remember that diagnostic decisions regarding the need for a biopsy should take into account all clinical variables and the overall PI-RADS imaging assessment.

2.4. Nonsuspicious mpMRI (PI-RADS categories 1 and 2)

Circumscribed low-signal or mixed-signal (encapsulated) nodules on T2WI represent normal BPH (PI-RADS 1; Fig. 1). Protruding or exophytic BPH nodules can occasionally be found in the PZ, often without continuity with BPH within the TZ [12,36–38]. In these cases, interpretation can be difficult. Assessment of the other T2WI planes (coronal and sagittal) can aid in verifying its nature. The most common benign abnormality in the PZ is acute or chronic prostatitis (PI-RADS 2). Prostatitis appears as a nonfocal intermediate signal on the ADC map, often with concurrent diffuse enhancement on DCE-MRI (Fig. 2). Postprostatitis scar tissue has a wedge-shaped or band-like appearance.

Recent prospective, multicenter trials show that mpMRI can obviate unnecessary biopsies by 21–49% in biopsy-naïve men [39–42]. Reported negative mpMRI lesions (PI-RADS 1–2 lesions) should be assessed by the urologist in combination with other clinical parameters and, if deemed necessary, discussed at multidisciplinary team (MDT) meeting. Results from an expert prostate MRI center show

that in only 3%, csPCa was found by a systematic biopsy (SB; predominantly International Society of Urological Pathology [ISUP] grade 2) in men with nonsuspicious mpMRI [41]. Therefore, a "safety net" was provided—a half-yearly PSA test. After 1 yr of follow-up, an additional 1% of csPCa was found, resulting in an mpMRI-negative predictive value (NPV) of 96%. This final 4% figure of false negatives is lower than the recent Cochrane systematic review average (8%), 5% of which are ISUP grade 2 and 3% ISUP grade ≥3, reflecting the expertise of central readings [43].

Regardless, it is clear that template mapping biopsies remains the "gold standard" for the likely pathologic state of the disease. The Cochrane systematic review also analyzed the performance of MRI with template mapping biopsies as a reference standard. The pooled NPV for csPCa (ISUP grade ≥2, prevalence of 30%) was 91% (95% confidence interval: 86–94%) [44]. The PROMIS trial also used transperineal template mapping biopsies and found a lower NPV (76%) [40]. The difference between the pooled and PROMIS data might be attributable to multiple factors including (imaging on 1.5 T MRI and nonadherence to PI-RADS v2 recommendations for imaging), clinical Likert score rather than rule-based imaging PI-RADS assessments, and/or a higher csPCa prevalence [7].

Therefore, when there is a high clinical suspicion of csPCa and negative mpMRI, an SB should be considered and should be discussed with the patient as part of shared decision making [45]. Men with negative mpMRI without a high clinical suspicion (eg, low PSAd) need not undergo immediate biopsy and be safely discharged to their general practitioner (GP), if an adequate safety net of PSA surveillance is implemented, with roles and responsibilities being clearly defined [41,46–48]. Our approach is to advise patients with negative MRI scans who do not undergo immediate biopsy to have 6-monthly PSA tests. If clinical suspicion persists, a re-referral for repeat MRI or an SB should be made.

2.5. Equivocal mpMRI (PI-RADS category 3)

Prevalence rates of PI-RADS 3 assessment in biopsy-naïve men varies between 6% and 39% [41,49]. It is reported that experienced readers have significantly lower rates of PI-RADS 3 scores; thus, the percentage of PI-RADS 3 scorings can be an indicator of reader quality [50]. Radiologic reviews at MDT meetings of equivocal lesions often showed up- or downgrade reclassification [51]. On an individual patient basis, each PI-RADS 3 lesion should be discussed at MDT meetings.

Equivocal lesions pose a diagnostic challenge because even though the proportion of csPCa in this group is low, a considerable percentage of men still have csPCa. The prevalence of csPCa (defined as ISUP grade ≥2) in this category is 4–27% [41,49,52–54]. Similar to PI-RADS 1–2 lesions, clinical risk stratification parameters can aid in decision making on the need to perform a biopsy or rather follow up the lesion with repeated mpMRI and repeated PSA measurements. Elevated PSAd (eg, ≥0.15 ng/ml/ml) has been demonstrated to predict the presence of csPCa for PI-RADS 3 lesions [53–58]. Blood-based and urinary biomarker–incorporated risk models might improve risk stratification, but there is currently insufficient information to advice on the optimal strategy of these men. When decisions are made not to biopsy men with PI-RADS 3 lesions, a "safety net" of imaging and PSA surveillance similar to PI-RADS 1–2 category should be implemented with urologic clinic follow-up (as opposed to GP).

2.6. Suspicious mpMRI (PI-RADS categories 4 and 5)

Using PI-RADS v2, mpMRI can predict the presence of csPCa with high diagnostic accuracy [41,59,60]. On average, in biopsy-naïve men, csPCa (ISUP grade ≥2) is diagnosed in 32–60% for PI-RADS category 4 and 67–83% for PI-RADS category 5 [39,41,42,48,49,54,61,62]. Therefore, PI-RADS 4–5 lesions should always be considered for biopsy if patients are likely to be treated. Whether to perform an SB in addition to an MRDB or only a targeted MRDB in biopsy-naïve men is still debated [47]. The most recent European Association of Urology guideline recommended performing an SB in addition to an MRDB [2]. This approach is supported by a growing body of evidence showing increasing yields with the combined approach in biopsy-naïve men (but not after a prior negative biopsy) [42,63–69]. However, a "focal saturation" approach (ie, multiple cores per suspicious lesion) has been proposed by the PI-RADS Steering Committee as an alternative, which might show similar detection rates of csPCa with the advantages of reducing the detection rates of low-grade PCa and the number of biopsy cores [41,70–74]. In the repeat-biopsy setting, the European and American urological guidelines recommend a target biopsy (in case of PI-RADS scores ≥3), or a case-specific decision, respectively [2,75].

Current literature does not show a significant advantage of one targeted biopsy technique over the others [54,76,77]. However, it should be remembered that these studies were not sufficiently powered to detect differences between techniques for lesions at different locations and by size. Therefore, MR in-bore guided, MR-transrectal ultrasound fusion, or cognitive biopsies can be performed with due consideration of lesion characteristics (size and location), equipment availability, and operators' preference.

Biopsy methods and histopathologic findings should be discussed at MDT meetings attended by radiologists, urologists, and pathologists. Radiologic-pathologic correlations must be performed, and in case of csPCa, appropriate metastatic imaging techniques can be selected according to risk status. Suspicious mpMRI lesions with negative explanatory pathology/low-grade cancer must be re-evaluated, and follow-up with PSA/mpMRI or repeat biopsy should be discussed [12,38]. Insufficient mpMRI quality and reader performance, inaccurate targeting of lesions (sampling error), or undersampling can attribute to undetected csPCa or risk-classification errors [78,79]. False-positive mpMRI (eg, granulomatous prostatitis and reader error) can also occur. In a large retrospective study, follow-up of patients with a negative biopsy after suspicious mpMRI

resulted in the detection of csPCa (defined as ISUP grade ≥2) in 1.7% of men [35].

3. Limitations, challenges, and future developments

Implementation of mpMRI as a triage test before prostate biopsy in biopsy-naïve men has its challenges. Studies showed that mpMRI as triage test is a cost-effective diagnostic approach; however, this is highly dependent on the quality of mpMRI (subsequent MRDB) and health care system [80–82]. PI-RADS (v2) improved standardization of image acquisition and reporting of mpMRI [59,60,83]. However, there remains considerable variation in inter-reader reproducibility, but this is highly dependent on radiologists' experience and training [41,84–88]. Whether the recently published PI-RADS v2.1 improves this needs to be investigated. An appropriate education program, with quality control, is needed for radiologists and urologists. With high-quality standard image acquisition and reading, the proportion of nonsuspicious mpMRI (PI-RADS 1–2) will increase and the number of equivocal lesions will reduce [50,89], although this also is dependent on the csPCa prevalence.

Furthermore, MDT meetings are crucial to discuss radiologic (eg, double read) and histopathologic findings, diagnostic decision making, and choice of an adequate safety net. Prebiopsy multivariate risk stratification using risk calculators, which include PI-RADS, clinical data, pathology, and genomics, needs to be developed and validated. Moreover, guideline recommendations for clinical decision making for each PI-RADS v2.1 category and subsequent biopsy results are needed. Availability and capacity of mpMRI and dedicated radiologists can limit the availability of mpMRI in daily clinical practice [45]. To shorten examination time, biparametric MRI (ie, omitting DCE-MRI) to exclude csPCa in biopsy-naïve men is increasingly being investigated, with promising initial results [90–92]. Biparametric MRI could reduce scan times and save cost for contrast agent injection, but data of prospective multireader trials in nonexpert centers are missing to routinely recommend this approach.

4. Conclusions

In addition to the previous "surgery-in-motion" video that shows how optimal mpMR images are acquired, this video also shows how the radiologists perform their interpretations. To enhance standardization, lesions must be scored using the PI-RADS assessment system. TZ lesions that show "erased charcoal" or disruption of "organized chaos," and PZ lesions that are "black" on the ADC map and "white" on the high *b*-value DWI should be evaluated for a likelihood of csPCa using the PI-RADS system. When mpMRI is of good quality and is evaluated according to the PI-RADS v2.1 recommendations, this technique adds valuable information to other clinical data and can be used to reliably exclude csPCa, and so to avoid a biopsy and indicate where MRDB cores should be targeted. The next video discusses these biopsy options (MR-targeted biopsy video).

***Author contributions*:** Jelle O. Barentsz had full access to all the data in the study and takes responsibility for the integrity of the data and the accuracy of the data analysis.

Study concept and design: Israël, van der Leest, Sedelaar, Padhani, Zámecnik, Barentsz.
Acquisition of data: Israël, van der Leest, Barentsz.
Analysis and interpretation of data: Israël, van der Leest, Sedelaar, Padhani, Zámecnik, Barentsz.
Drafting of the manuscript: Israël, van der Leest, Barentsz.
Critical revision of the manuscript for important intellectual content: Israël, van der Leest, Sedelaar, Padhani, Zámecnik, Barentsz.
Statistical analysis: Israël, van der Leest, Sedelaar, Padhani, Zámecnik, Barentsz.
Obtaining funding: None.
Administrative, technical, or material support: Barentsz.
Supervision: Barentsz.
Other: None.

Financial disclosures: Jelle O. Barentsz certifies that all conflicts of interest, including specific financial interests and relationships and affiliations relevant to the subject matter or materials discussed in the manuscript (eg, employment/affiliation, grants or funding, consultancies, honoraria, stock ownership or options, expert testimony, royalties, or patents filed, received, or pending), are the following: None.

***Funding/Support and role of the sponsor*:** This work was supported by Soteria Medical.

***Acknowledgments*:** We like to thank Soteria Medical (Arnhem, the Netherlands) for their assistance in producing the video.

Appendix A. Supplementary data

Supplementary material related to this article can be found, in the online version, at doi:https://doi.org/10.1016/j.eururo.2019.10.024.

References

[1] Hricak H, Choyke PL, Eberhardt SC, Leibel SA, Scardino PT. Imaging prostate cancer: a multidisciplinary perspective. Radiology 2007;243:28–53.
[2] Mottet N, van den Bergh RCN, Briers E, et al. EAU – ESTRO – ESUR – SIOG guidelines on prostate cancer 2019. In: European Association of Urology guidelines, editor. Presented at the EAU Annual Congress Barcelona 2019. Arnhem, The Netherlands: European Association of Urology Guidelines Office; 2019.
[3] Briganti A, Fossati N, Catto JWF, et al. Active surveillance for low-risk prostate cancer: the European Association of Urology position in 2018. Eur Urol 2018;74:357–68.
[4] Kitajima K, Hartman RP, Froemming AT, Hagen CE, Takahashi N, Kawashima A. Detection of local recurrence of prostate cancer after radical prostatectomy using endorectal coil MRI at 3 T: addition of DWI and dynamic contrast enhancement to T2-weighted MRI. AJR Am J Roentgenol 2015;205:807–16.

[5] Schmidt MA, Payne GS. Radiotherapy planning using MRI. Phys Med Biol 2015;60:R323–61.
[6] Ko YH, Song PH, Moon KH, Jung HC, Cheon J, Sung DJ. The optimal timing of post-prostate biopsy magnetic resonance imaging to guide nerve-sparing surgery. Asian J Androl 2014;16:280–4.
[7] Weinreb JC, Barentsz JO, Choyke PL, et al. PI-RADS Prostate Imaging - Reporting and Data System: 2015, version 2. Eur Urol 2016;69:16–40.
[8] Walz J, Epstein JI, Ganzer R, et al. A critical analysis of the current knowledge of surgical anatomy of the prostate related to optimisation of cancer control and preservation of continence and erection in candidates for radical prostatectomy: an update. Eur Urol 2016;70:301–11.
[9] Chen ME, Johnston DA, Tang K, Babaian RJ, Troncoso P. Detailed mapping of prostate carcinoma foci: biopsy strategy implications. Cancer 2000;89:1800–9.
[10] McNeal JE, Redwine EA, Freiha FS, Stamey TA. Zonal distribution of prostatic adenocarcinoma. Correlation with histologic pattern and direction of spread. Am J Surg Pathol 1988;12:897–906.
[11] Akin O, Sala E, Moskowitz CS, et al. Transition zone prostate cancers: features, detection, localization, and staging at endorectal MR imaging. Radiology 2006;239:784–92.
[12] Rosenkrantz AB, Taneja SS. Radiologist, be aware: ten pitfalls that confound the interpretation of multiparametric prostate MRI. AJR Am J Roentgenol 2014;202:109–20.
[13] Panebianco V, Giganti F, Kitzing YX, et al. An update of pitfalls in prostate mpMRI: a practical approach through the lens of PI-RADS v. 2 guidelines. Insights Imaging 2018;9:87–101.
[14] Barentsz JO, Richenberg J, Clements R, et al. ESUR prostate MR guidelines 2012. Eur Radiol 2012;22:746–57.
[15] Barentsz JO, Weinreb JC, Verma S, et al. Synopsis of the PI-RADS v2 guidelines for multiparametric prostate magnetic resonance imaging and recommendations for use. Eur Urol 2016;69:41–9.
[16] Ren J, Huan Y, Wang H, et al. Diffusion-weighted imaging in normal prostate and differential diagnosis of prostate diseases. Abdom Imaging 2008;33:724–8.
[17] Hambrock T, Somford DM, Huisman HJ, et al. Relationship between apparent diffusion coefficients at 3.0-T MR imaging and Gleason grade in peripheral zone prostate cancer. Radiology 2011;259:453–61.
[18] Downes MR, Gibson E, Sykes J, Haider M, van der Kwast TH, Ward A. Determination of the association between T2-weighted MRI and Gleason sub-pattern: a proof of principle study. Acad Radiol 2016;23:1412–21.
[19] De Visschere PJ, Vral A, Perletti G, et al. Multiparametric magnetic resonance imaging characteristics of normal, benign and malignant conditions in the prostate. Eur Radiol 2017;27:2095–109.
[20] Qayyum A. Diffusion-weighted imaging in the abdomen and pelvis: concepts and applications. Radiographics 2009;29:1797–810.
[21] Langer DL, van der Kwast TH, Evans AJ, et al. Prostate tissue composition and MR measurements: investigating the relationships between ADC, T2, K(trans), v(e), and corresponding histologic features. Radiology 2010;255:485–94.
[22] Feuerlein S, Davenport MS, Krishnaraj A, Merkle EM, Gupta RT. Computed high b-value diffusion-weighted imaging improves lesion contrast and conspicuity in prostate cancer. Prostate Cancer Prostatic Dis 2015;18:155–60.
[23] Wetter A, Nensa F, Lipponer C, et al. High and ultra-high b-value diffusion-weighted imaging in prostate cancer: a quantitative analysis. Acta Radiol 2015;56:1009–15.
[24] Kim JH, Kim JK, Park BW, Kim N, Cho KS. Apparent diffusion coefficient: prostate cancer versus noncancerous tissue according to anatomical region. J Magn Reson Imaging 2008;28:1173–9.
[25] Tamada T, Sone T, Toshimitsu S, et al. Age-related and zonal anatomical changes of apparent diffusion coefficient values in normal human prostatic tissues. J Magn Reson Imaging 2008;27:552–6.
[26] Turkbey B, Shah VP, Pang Y, et al. Is apparent diffusion coefficient associated with clinical risk scores for prostate cancers that are visible on 3-T MR images? Radiology 2011;258:488–95.
[27] Boesen L, Chabanova E, Logager V, Balslev I, Thomsen HS. Apparent diffusion coefficient ratio correlates significantly with prostate cancer Gleason score at final pathology. J Magn Reson Imaging 2015;42:446–53.
[28] Hambrock T, Hoeks C, Hulsbergen-van de Kaa C, et al. Prospective assessment of prostate cancer aggressiveness using 3-T diffusion-weighted magnetic resonance imaging-guided biopsies versus a systematic 10-core transrectal ultrasound prostate biopsy cohort. Eur Urol 2012;61:177–84.
[29] Oto A, Kayhan A, Jiang Y, et al. Prostate cancer: differentiation of central gland cancer from benign prostatic hyperplasia by using diffusion-weighted and dynamic contrast-enhanced MR imaging. Radiology 2010;257:715–23.
[30] Verma S, Turkbey B, Muradyan N, et al. Overview of dynamic contrast-enhanced MRI in prostate cancer diagnosis and management. AJR Am J Roentgenol 2012;198:1277–88.
[31] Huisman HJ, Engelbrecht MR, Barentsz JO. Accurate estimation of pharmacokinetic contrast-enhanced dynamic MRI parameters of the prostate. J Magn Reson Imaging 2001;13:607–14.
[32] Oppenheimer DC, Weinberg EP, Hollenberg GM, Meyers SP. Multiparametric magnetic resonance imaging of recurrent prostate cancer. J Clin Imaging Sci 2016;6:18.
[33] Barrett T, Vargas HA, Akin O, Goldman DA, Hricak H. Value of the hemorrhage exclusion sign on T1-weighted prostate MR images for the detection of prostate cancer. Radiology 2012;263:751–7.
[34] Turkbey B, Rosenkrantz AB, Haider MA, et al. Prostate Imaging Reporting and Data System Version 2.1: 2019 update of Prostate Imaging Reporting and Data System Version 2. Eur Urol 2019;76:340–51.
[35] Venderink W, van Luijtelaar A, Bomers JG, et al. Results of targeted biopsy in men with magnetic resonance imaging lesions classified equivocal, likely or highly likely to be clinically significant prostate cancer. Eur Urol 2017;73:353–60.
[36] Li Y, Mongan J, Behr SC, et al. Beyond prostate adenocarcinoma: expanding the differential diagnosis in prostate pathologic conditions. Radiographics 2016;36:1055–75.
[37] Panebianco V, Barchetti F, Barentsz J, et al. Pitfalls in interpreting mp-MRI of the prostate: a pictorial review with pathologic correlation. Insights Imaging 2015;6:611–30.
[38] Kitzing YX, Prando A, Varol C, Karczmar GS, Maclean F, Oto A. Benign conditions that mimic prostate carcinoma: MR imaging features with histopathologic correlation. Radiographics 2016;36:162–75.
[39] Kasivisvanathan V, Rannikko AS, Borghi M, et al. MRI-targeted or standard biopsy for prostate-cancer diagnosis. N Engl J Med 2018;378:1767–77.
[40] Ahmed HU, El-Shater Bosaily A, Brown LC, et al. Diagnostic accuracy of multi-parametric MRI and TRUS biopsy in prostate cancer (PROMIS): a paired validating confirmatory study. Lancet 2017;389:815–22.
[41] van der Leest M, Cornel E, Israel B, et al. Head-to-head comparison of transrectal ultrasound-guided prostate biopsy versus multiparametric prostate resonance imaging with subsequent magnetic resonance-guided biopsy in biopsy-naive men with elevated prostate-specific antigen: a large prospective multicenter clinical study. Eur Urol 2019;75:570–8.
[42] Rouviere O, Puech P, Renard-Penna R, et al. Use of prostate systematic and targeted biopsy on the basis of multiparametric MRI in

biopsy-naive patients (MRI-FIRST): a prospective, multicentre, paired diagnostic study. Lancet Oncol 2019;20:100–9.
[43] Drost FH, Osses DF, Nieboer D, et al. Prostate MRI, with or without MRI-targeted biopsy, and systematic biopsy for detecting prostate cancer. Cochrane Database Syst Rev 2019;4:CD012663.
[44] Drost FH, Osses D, Nieboer D , et al. Prostate magnetic resonance imaging, with or without magnetic resonance imaging-targeted biopsy, and systematic biopsy for detecting prostate cancer: a Cochrane systematic review and meta-analysis. Eur Urol 2020;77:78–94.
[45] Padhani AR, Weinreb J, Rosenkrantz AB, Villeirs G, Turkbey B, Barentsz J. Prostate Imaging-Reporting and Data System Steering Committee: PI-RADS v2 status update and future directions. Eur Urol 2019;75:385–96.
[46] Oishi M, Shin T, Ohe C, et al. Which patients with negative magnetic resonance imaging can safely avoid biopsy for prostate cancer? J Urol 2019;201:268–77.
[47] Brizmohun Appayya M, Adshead J, Ahmed HU, et al. National implementation of multi-parametric magnetic resonance imaging for prostate cancer detection—recommendations from a UK consensus meeting. BJU Int 2018;122:13–25.
[48] Panebianco V, Barchetti G, Simone G, et al. Negative multiparametric magnetic resonance imaging for prostate cancer: what's next? Eur Urol 2018;74:48–54.
[49] Schoots IG. MRI in early prostate cancer detection: how to manage indeterminate or equivocal PI-RADS 3 lesions? Transl Androl Urol 2018;7:70–82.
[50] Greer MD, Brown AM, Shih JH, et al. Accuracy and agreement of PIRADSv2 for prostate cancer mpMRI: A multireader study. J Magn Reson Imaging 2017;45:579–85.
[51] Steinkohl F, Gruber L, Bektic J, et al. Retrospective analysis of the development of PIRADS 3 lesions over time: when is a follow-up MRI reasonable? World J Urol 2018;36:367–73.
[52] Sheridan AD, Nath SK, Syed JS, et al. Risk of clinically significant prostate cancer associated with Prostate Imaging Reporting and Data System category 3 (equivocal) lesions identified on multiparametric prostate MRI. AJR Am J Roentgenol 2018;210:347–357.
[53] Ullrich T, Quentin M, Arsov C, et al. Risk stratification of equivocal lesions on multiparametric magnetic resonance imaging of the prostate. J Urol 2018;199:691–8.
[54] Venderink W, van der Leest M, van Luijtelaar A, et al. Retrospective comparison of direct in-bore magnetic resonance imaging (MRI)-guided biopsy and fusion-guided biopsy in patients with MRI lesions which are likely or highly likely to be clinically significant prostate cancer. World J Urol 2017;35:1849–55.
[55] Brizmohun Appayya M, Sidhu HS, Dikaios N, et al. Characterizing indeterminate (Likert-score 3/5) peripheral zone prostate lesions with PSA density, PI-RADS scoring and qualitative descriptors on multiparametric MRI. Br J Radiol 2018;91:20170645.
[56] Washino S, Okochi T, Saito K, et al. Combination of Prostate Imaging Reporting and Data System (PI-RADS) score and prostate-specific antigen (PSA) density predicts biopsy outcome in prostate biopsy naive patients. BJU Int 2017;119:225–33.
[57] Rais-Bahrami S, Siddiqui MM, Vourganti S, et al. Diagnostic value of biparametric magnetic resonance imaging (MRI) as an adjunct to prostate-specific antigen (PSA)-based detection of prostate cancer in men without prior biopsies. BJU Int 2015;115:381–8.
[58] Felker ER, Raman SS, Margolis DJ, et al. Risk stratification among men with Prostate Imaging Reporting and Data System version 2 category 3 transition zone lesions: is biopsy always necessary? AJR Am J Roentgenol 2017;209:1272–7.
[59] Zhang L, Tang M, Chen S, Lei X, Zhang X, Huan Y. A meta-analysis of use of Prostate Imaging Reporting and Data System version 2 (PI-RADS V2) with multiparametric MR imaging for the detection of prostate cancer. Eur Radiol 2017;27:5204–14.
[60] Woo S, Suh CH, Kim SY, Cho JY, Kim SH. Diagnostic Performance of Prostate Imaging Reporting and Data System Version 2 for detection of prostate cancer: a systematic review and diagnostic meta-analysis. Eur Urol 2017;72:177–88.
[61] Mehralivand S, Bednarova S, Shih JH, et al. Prospective evaluation of PI-RADS version 2 using the International Society of Urological Pathology Prostate Cancer Grade Group system. J Urol 2017;198:583–90.
[62] Moldovan PC, Van den Broeck T, Sylvester R, et al. What is the negative predictive value of multiparametric magnetic resonance imaging in excluding prostate cancer at biopsy? A systematic review and meta-analysis from the European Association of Urology Prostate Cancer Guidelines Panel. Eur Urol 2017;72:250–66.
[63] Maxeiner A, Kittner B, Blobel C, et al. Primary magnetic resonance imaging/ultrasonography fusion-guided biopsy of the prostate. BJU Int 2018;122:211–8.
[64] Ploussard G, Borgmann H, Briganti A, et al. Positive pre-biopsy MRI: are systematic biopsies still useful in addition to targeted biopsies? World J Urol 2019;37(2):243–51.
[65] Washino S, Kobayashi S, Okochi T, et al. Cancer detection rate of prebiopsy MRI with subsequent systematic and targeted biopsy are superior to non-targeting systematic biopsy without MRI in biopsy naive patients: a retrospective cohort study. BMC Urol 2018;18:51.
[66] Hansen NL, Barrett T, Kesch C, et al. Multicentre evaluation of magnetic resonance imaging supported transperineal prostate biopsy in biopsy-naive men with suspicion of prostate cancer. BJU Int 2018;122:40–9.
[67] Radtke JP, Schwab C, Wolf MB, et al. Multiparametric magnetic resonance imaging (MRI) and MRI-transrectal ultrasound fusion biopsy for index tumor detection: correlation with radical prostatectomy specimen. Eur Urol 2016;70:846–53.
[68] Hofbauer SL, Maxeiner A, Kittner B, et al. Validation of Prostate Imaging Reporting and Data System version 2 for the detection of prostate cancer. J Urol 2018;200:767–73.
[69] Stabile A, Giganti F, Emberton M, Moore CM. MRI in prostate cancer diagnosis: do we need to add standard sampling? A review of the last 5 years. Prostate Cancer Prostatic Dis 2018;21:473–87.
[70] Calio BP, Sidana A, Sugano D, et al. Risk of upgrading from prostate biopsy to radical prostatectomy pathology—does saturation biopsy of index lesion during multiparametric magnetic resonance imaging-transrectal ultrasound fusion biopsy help? J Urol 2018;199:976–82.
[71] Muthigi A, George AK, Sidana A, et al. Missing the mark: prostate cancer upgrading by systematic biopsy over magnetic resonance imaging/transrectal ultrasound fusion biopsy. J Urol 2017;197:327–34.
[72] Lu AJ, Syed JS, Ghabili K, et al. Role of core number and location in targeted magnetic resonance imaging-ultrasound fusion prostate biopsy. Eur Urol 2019;76:14–7.
[73] Zhang M, Milot L, Khalvati F, et al. Value of increasing biopsy cores per target with cognitive MRI-targeted transrectal US prostate biopsy. Radiology 2019;291:83–9.
[74] Padhani AR, Barentsz J, Villeirs G, et al. PI-RADS Steering Committee: the PI-RADS multiparametric MRI and MRI-directed biopsy pathway. Radiology 2019;292:464–74.
[75] Rosenkrantz AB, Verma S, Choyke P, et al. Prostate magnetic resonance imaging and magnetic resonance imaging targeted biopsy in patients with a prior negative biopsy: a consensus statement by AUA and SAR. J Urol 2016;196:1613–8.
[76] Wegelin O, van Melick HHE, Hooft L, et al. Comparing three different techniques for magnetic resonance imaging-targeted prostate biopsies: a systematic review of in-bore versus magnetic resonance

imaging-transrectal ultrasound fusion versus cognitive registration. Is there a preferred technique? Eur Urol 2017;71:517–31.
[77] Wegelin O, Exterkate L, van der Leest M, et al. The FUTURE trial: a multicenter randomised controlled trial on target biopsy techniques based on magnetic resonance imaging in the diagnosis of prostate cancer in patients with prior negative biopsies. Eur Urol 2019;75:582–90.
[78] Kenigsberg AP, Renson A, Rosenkrantz AB, et al. Optimizing the number of cores targeted during prostate magnetic resonance imaging fusion target biopsy. Eur Urol Oncol 2018;1:418–25.
[79] Porpiglia F, De Luca S, Passera R, et al. Multiparametric magnetic resonance/ultrasound fusion prostate biopsy: number and spatial distribution of cores for better index tumor detection and characterization. J Urol 2017;198:58–64.
[80] Pahwa S, Schiltz NK, Ponsky LE, Lu Z, Griswold MA, Gulani V. Cost-effectiveness of MR imaging-guided strategies for detection of prostate cancer in biopsy-naive men. Radiology 2017;285:157–66.
[81] Faria R, Soares MO, Spackman E, et al. optimising the diagnosis of prostate cancer in the era of multiparametric magnetic resonance imaging: a cost-effectiveness analysis based on the Prostate MR Imaging Study (PROMIS). Eur Urol 2018;73:23–30.
[82] de Rooij M, Crienen S, Witjes JA, Barentsz JO, Rovers MM, Grutters JP. Cost-effectiveness of magnetic resonance (MR) imaging and MR-guided targeted biopsy versus systematic transrectal ultrasound-guided biopsy in diagnosing prostate cancer: a modelling study from a health care perspective. Eur Urol 2014;66:430–6.
[83] Chen F, Cen S, Palmer S. Application of Prostate Imaging Reporting and Data System version 2 (PI-RADS v2): interobserver agreement and positive predictive value for localization of intermediate- and high-grade prostate cancers on multiparametric magnetic resonance imaging. Acad Radiol 2017;24:1101–6.
[84] Glazer DI, Mayo-Smith WW, Sainani NI, et al. Interreader agreement of Prostate Imaging Reporting and Data System version 2 using an in-bore MRI-guided prostate biopsy cohort: a single institution's initial experience. AJR Am J Roentgenol 2017;209:W145–51.
[85] Rosenkrantz AB, Ginocchio LA, Cornfeld D, et al. Interobserver reproducibility of the PI-RADS version 2 lexicon: a multicenter study of six experienced prostate radiologists. Radiology 2016;280:793–804.
[86] Shankar PR, Kaza RK, Al-Hawary MM, et al. Impact of clinical history on maximum PI-RADS version 2 score: a six-reader 120-case sham history retrospective evaluation. Radiology 2018;288:158–63.
[87] Purysko AS, Bittencourt LK, Bullen JA, Mostardeiro TR, Herts BR, Klein EA. Accuracy and interobserver agreement for Prostate Imaging Reporting and Data System, version 2, for the characterization of lesions identified on multiparametric MRI of the prostate. AJR Am J Roentgenol 2017;209:339–49.
[88] Mussi TC, Yamauchi FI, Tridente CF, et al. Interobserver agreement and positivity of PI-RADS version 2 among radiologists with different levels of experience. Acad Radiol 2019;26:1017–22.
[89] Garcia-Reyes K, Passoni NM, Palmeri ML, et al. Detection of prostate cancer with multiparametric MRI (mpMRI): effect of dedicated reader education on accuracy and confidence of index and anterior cancer diagnosis. Abdom Imaging 2015;40:134–42.
[90] Woo S, Suh CH, Kim SY, Cho JY, Kim SH, Moon MH. Head-to-Head comparison between biparametric and multiparametric MRI for the diagnosis of prostate cancer: a systematic review and meta-analysis. AJR Am J Roentgenol 2018;211:W226–41.
[91] Boesen L, Norgaard N, Logager V, et al. Assessment of the diagnostic accuracy of biparametric magnetic resonance imaging for prostate cancer in biopsy-naive men: the Biparametric MRI for Detection of Prostate Cancer (BIDOC) study. JAMA Netw Open 2018;1:e180219.
[92] van der Leest M, Israel B, Cornel EB, et al. High diagnostic performance of short magnetic resonance imaging protocols for prostate cancer detection in biopsy-naive men: the next step in magnetic resonance imaging accessibility. Eur Urol 2019;76:574–81.

EUROPEAN UROLOGY 77 (2020) 481–490

available at www.sciencedirect.com
journal homepage: www.europeanurology.com

European Association of Urology

Surgery in Motion

Multiparametric Magnetic Resonance Imaging for the Detection of Clinically Significant Prostate Cancer: What Urologists Need to Know. Part 3: Targeted Biopsy

Wulphert Venderink[a], *Joyce G. Bomers*[a], *Christiaan G. Overduin*[a], *Anwar R. Padhani*[b], *Gijs R. de Lauw*[a], *Michiel J. Sedelaar*[a], *Jelle O. Barentsz*[a,*]

[a] *Department of Radiology, Radboud University Nijmegen Medical Center, Nijmegen, The Netherlands;* [b] *Paul Strickland Scanner Centre, Northwood, UK*

Article info

Article history:
Accepted October 18, 2019

Associate Editor:
Alexandre Mottrie

Keywords:
Prostate cancer
Multiparametric magnetic resonance imaging
Prostate Imaging Reporting and Data System
Prostate Imaging Reporting and Data System version 2
Magnetic resonance–guided biopsy
Prostate biopsy

Please visit www.europeanurology.com and www.urosource.com to view the accompanying video.

Abstract

Background: After a lesion has been assessed adequately on multiparametric magnetic resonance imaging (mpMRI), magnetic resonance (MR)-guided biopsy (MRGB) is the logical next step. The choice of the MRGB technique, however, is difficult.
Objective: To show the advantages and disadvantages of the three commonly used MRGB techniques—MRI-ultrasound fusion MRGB (fus-MRGB), direct in-bore MRGB (inbore-MRGB), and cognitive MRGB (cog-MRGB), and to determine when each of the techniques can be used.
Design, setting, and participants: Based on expert opinion and literature overview, the advantages, disadvantages, and challenges of fus-MRGB, inbore-MRGB, and cog-MRGB are evaluated. Further, the clinical setting of each biopsy strategy is assessed.
Surgical procedure: Based on expert opinion and literature data, the three biopsy procedures are evaluated, and the important pros and cons are determined.
Measurements: The basic concept of each biopsy technique is reviewed, which would result in a clinical recommendation. This will be shown in individual patients.
Results and limitations: The accompanying video shows how fus-MRGB and inbore-MRGB are performed in our hospital. An important advantage of fus-MRGB is its generally availability; however, it has fusion-error limitations. Although not supported by evidence, inbore-MRGB seems to be better suited for smaller lesions, but is rather expensive. Cog-MRGB is easy to use and inexpensive, but is more operator dependent as it requires knowledge about both ultrasound and MR images. Readers should be aware that our MRGB approach is largely based on expert opinion and, where possible, supported by evidence.
Conclusions: This article and the accompanying video show different MRGB techniques. The advantages and disadvantages of the three biopsy techniques, as well as the clinical setting in which each biopsy strategy is being used in our hospital, are discussed. Fus-MRGB is our first choice for prostate biopsy. Direct inbore-MRGB is used in difficult lesions but is mainly used as a "problem solver" (eg, a negative biopsy with a high suspicion for clinically significant prostate cancer). In our opinion, cog-MRGB is best for sampling larger and diffuse lesions.
Patient summary: This third surgery in motion contribution shows our approach in magnetic resonance (MR)-guided biopsy (MRGB). Fusion MRGB is our first choice for prostate biopsy. In-bore MRGB is used in selected, difficult cases, mainly as a problem solver. In our point of view, cognitive MRGB seems to be best for sampling larger lesions and diffuse processes.

* Corresponding author. Department of Radiology, Radboud University Nijmegen Medical Center, P.O. Box 9101, Nijmegen, The Netherlands. Tel. +31243619196, +31625015262; Fax: +31243540866.
E-mail address: jelle.barentsz@radboudumc.nl (J.O. Barentsz).

https://doi.org/10.1016/j.eururo.2019.10.009

1. Introduction

High-level evidence demonstrates that multiparametric magnetic resonance imaging (mpMRI) and subsequent magnetic resonance (MR) targeted biopsy (MRGB) are able to increase the detection of clinically significant prostate cancer (csPCa), while at the same time, decrease the detection of clinically insignificant prostate cancer (insignPCa) [1–5].

Although mpMRI is accurate in detecting and localising suspicious csPCa lesions, pathological confirmation is necessary to confirm a cancer diagnosis and assess cancer aggressiveness. Since the introduction of prostate mpMRI, several targeted biopsy strategies have emerged as options for precision diagnosis. In this manuscript, we will describe the advantages and disadvantages, and discuss the challenges of visual/cognitive targeted biopsy (cog-MRGB), software-assisted MRI-transrectal ultrasound (TRUS) fusion biopsy (fus-MRGB), and direct in-bore MRI targeted biopsy (inbore-MRGB). The clinical setting of patients that determines biopsy strategies will be discussed. The accompanying video briefly demonstrates how to perform MRGB and MRI-TRUS fusion biopsy.

2. MRI targeted biopsy

An important prerequisite for a successful MRGB starts with good-quality images and interpretations of mpMRI. These topics are described in the previous “surgery-in-motion” articles and videos [36,37].

All MRGB strategies have in common that mpMRI information is analysed and used to target one or more biopsy needles into a tumour suspicious region of interest (ROI). Since image postprocessing and reading of the images require time, the mpMRI and subsequent MRGB are usually performed in two separate sessions with gland and target delineations after image interpretations.

Suspicious lesion(s) identified on mpMRI can be targeted under either direct ultrasound or MRI guidance. With ultrasound guidance, there should be some combination of the information of the mpMRI and ultrasound images (image registration). This image registration can be done cognitively or with the help of registration software. In inbore-MRGB, near-real-time MR images are used to direct the biopsy needle towards the suspicious ROI. Thus, with inbore-MRGB, there is no need for image registration.

2.1. Cognitive MRI-ultrasound fusion

In cog-MRGB (visual targeted), the ultrasound operator simply directs the biopsy needle towards the suspicious lesion identified on MRI. The performing operator cognitively correlates the mpMRI- and the real-time TRUS images to sample the identified ROIs. To improve the biopsy accuracy, anatomical landmarks can be used as internal fiducials. Examples of such anatomical fiducials are benign prostatic hyperplasia (BPH) nodules, cysts or calcifications, gland contours, seminal vesicle position, urethra, etc. Such fiducials are often seen on both mpMRI and TRUS (Fig. 1). Cog-MRGB requires knowledge of appearances of cancers and prostatic structures on both TRUS and mpMRI. As cog-MRGB is usually performed by urologists, education of mpMRI interpretation, and gland and target contouring is important for success.

2.1.1. Disadvantages and advantages of cognitive fusion

Biopsy accuracy can be limited in the absence of internal fiducials, especially for smaller lesions located anteriorly, at the apex or the base of the prostate, where TRUS biopsy is known to be challenging (Fig. 2) [6]. Furthermore, there is no image confirmation that the biopsy was done accurately because cog-MRGB usually does not allow tracking and recording of biopsy and target coordinates.

There are additional important constraints of the cognitive fusion technique. Differences in patient positioning and the use of a rectal ultrasound probe can distort the anatomy and result in sampling error. Cog-MRGB requires good understanding and experience in reading of mpMRI and TRUS imaging in real time. Clear communication between radiologists and biopsy operators is mandatory, so that the biopsy operator knows which glandular region should be sampled. These challenges make cognitive fusion highly operator dependent [7] and challenging, often requiring additional biopsy cores to counteract targeting errors for smaller lesions.

The most important advantage of cog-MRGB is, however, that there is no need for specialised and often expensive registration software enabling deployment in the clinical routine. In addition, the performing operator can combine targeted biopsy and systematic TRUS biopsy in one session [3,8,9]. Unfortunately, published results of cog-MRGB show inconsistent results. Several studies demonstrated superiority versus systematic TRUS biopsy, while others showed that it is not better [10–14]. Moreover, a recently conducted multicentre randomised controlled trial by Wegelin et al [5], comparing the three MRGB strategies, was not able to end this discussion as it hampered underpowering.

2.1.2. Role of cognitive fusion (cog-MRGB)

In our opinion, based on the mentioned advantages and disadvantages in section 2.1.1, cog-MRGB seems to be most useful for sampling large lesions or diffuse abnormalities located at the peripheral zone of the prostate, where it continues to be a practical and lower-cost option. In many countries, without the availability of expensive fusion equipment, the introduction of cog-MRGB is potentially the first step-up in improving biopsy accuracy. Larger lesions and more aggressive cancers, especially located in an mpMRI T2-weighted (T2W)-hyperintense peripheral zone, can often easily be identified on the ultrasound images with prior mpMRI knowledge. In such cases, it is unnecessary to target such lesions with MRI-fusion techniques or inbore-MRGB. Fig. 3 represents a lesion that should definitely be biopsied with cog-MRGB. However, the introduction of a variety of fus-MRGB methods has resulted in a decline in the use of cog-MRGB fusion.

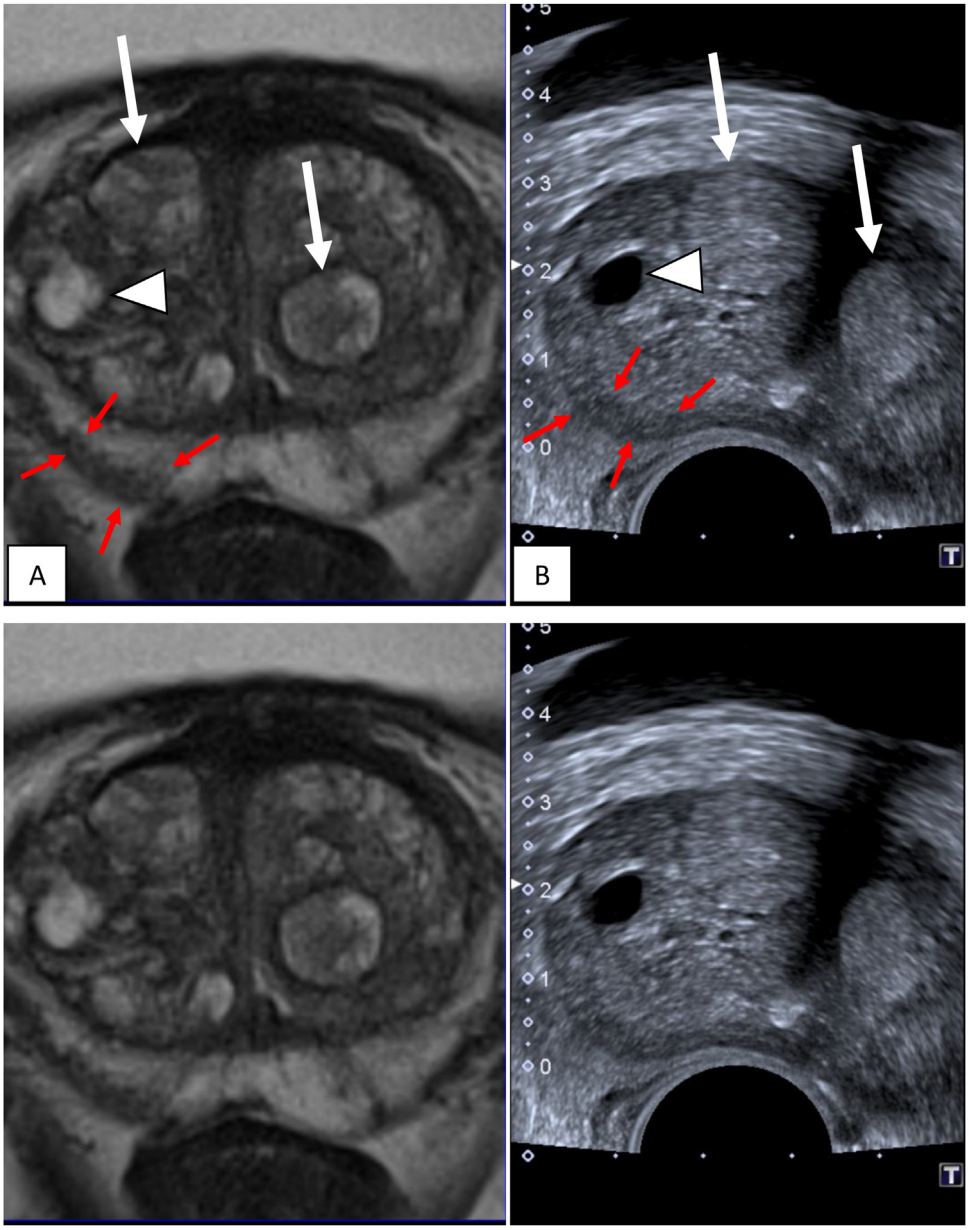

Fig. 1 – Internal fiducials seen on MRI and ultrasound. Example of internal fiducials in a 73-yr-old male (PSA 4.3 ng/ml), with a PZ PI-RADS 3 lesion at 7 o'clock (red arrows; score 3/3/–). These fiducials can be used for image registration for MRI-TRUS fusion or for cognitive fusion biopsy. (A) T2WI of a cyst (arrowhead) and two BPH nodules (white arrows) are seen. (B) US image of the cyst (arrowhead) and the BPH nodules (white arrows) are reproduced. The suspicious lesion is after fusion of the images also visible on ultrasound. This turned out to be prostatitis. BPH = benign prostatic hyperplasia; MRI = magnetic resonance imaging; PI-RADS = Prostate Imaging Reporting and Data System; PSA = prostate-specific antigen; PZ = peripheral zone; T2WI = T2-weighted image; TRUS = transrectal ultrasound; US = ultrasound.

2.2. MRI-TRUS fusion (fus-MRGB)

Working towards a more accurate biopsy strategy using MRI-TRUS fusion image registration, several manufacturers have introduced fusion software packages in the market. Using software-based platforms, previously obtained mpMRI information, often T2W images are fused with real-time TRUS images. As with cog-MRGB, the diagnostic mpMRI and the MRI-TRUS fusion biopsy are performed in separate sessions.

There are multiple implementations of fus-MRGB. Available systems differ, for example, in tracking mechanisms (eg, electromagnetic or mechanical arm), biopsy routes (eg, transperineal or transrectal), or the imaging overlay (eg, side by side or superimposed). The most important difference, however, is the use of the image registration algorithms being either rigid or elastic [15]. Owing to deformations of the prostate on TRUS, for example, caused by the introduction of the ultrasound probe or by bowel gas, adjustments are needed to

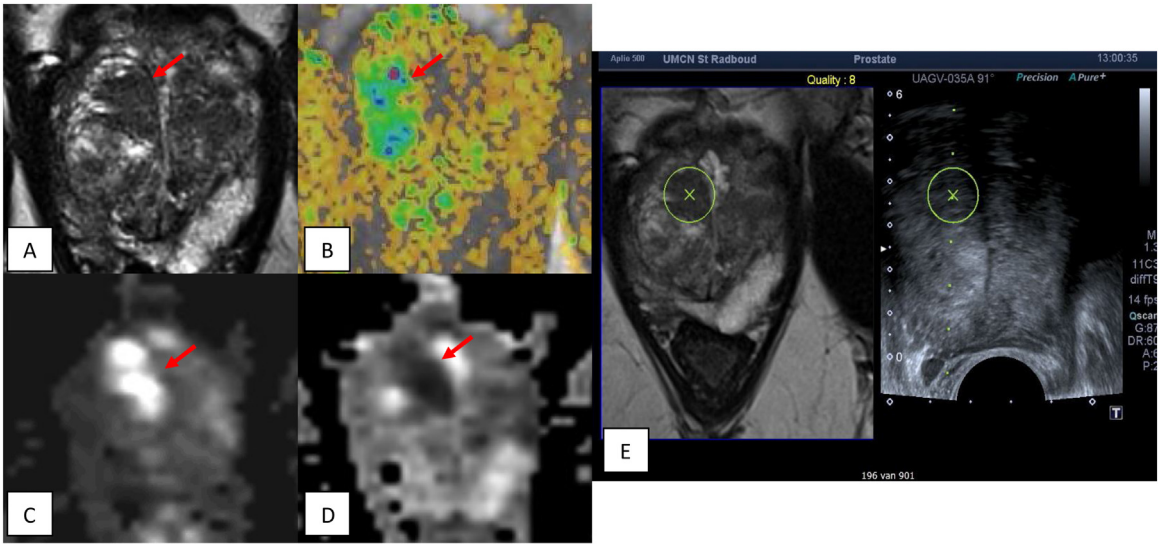

Fig. 2 – Lesion located anteriorly in prostate. A 67-yr-old male (PSA 8.9 ng/ml) with a PI-RADS 4 anterior TZ lesion at 11 o'clock (red arrows; score 4/4/+). After uploading T2WI on the ultrasound machine and coupling for MRI-TRUS fusion biopsy, the lesion was not visible on the ultrasound images (E). Now the operator needs to completely rely on the coupling software and biopsy of the region of interest within the green circle. Biopsy revealed Gleason 3 + 3 PCa. (A) T2WI. (B) DCE. (C) Calculated high *b*-value image. (D) Calculated ADC map. (E) MRI-TRUS fusion after rigid image registration. ADC = apparent diffusion coefficient; DCE = dynamic contrast enhanced; MRI = magnetic resonance imaging; PCa = prostate cancer; PI-RADS = Prostate Imaging Reporting and Data System; PSA = prostate-specific antigen; T2WI = T2-weighted image; TRUS = transrectal ultrasound; TZ = transition zone.

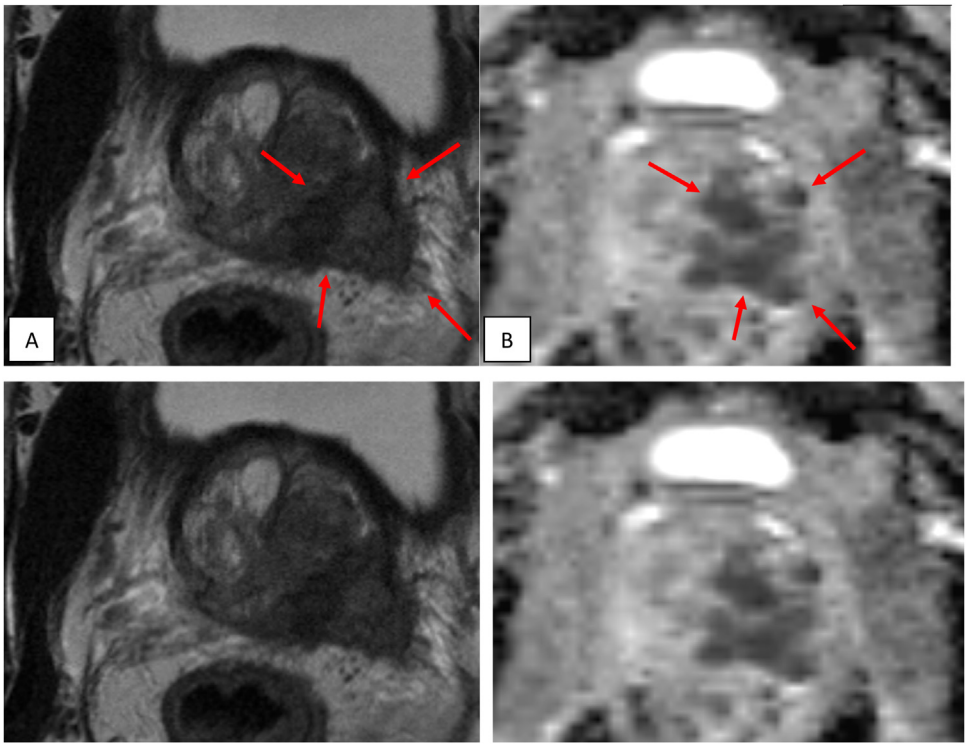

Fig. 3 – Prostate cancer affecting half of the prostate. A biopsy-naïve 63-yr-old male (PSA 21.0 ng/ml) with PI-RADS 5 lesion (score 5/5/+) covering the left half of prostate. Direct inbore-MRGB would be a waste of resources. Adequate sampling can be performed with cog- or fus-MRGB. This example is exceptional and prostate cancer would also be discovered by systematic TRUS biopsy. Fus-MRGB demonstrated Gleason 5 + 4 PCa. (A) T2WI. B) Calculated ADC map. ADC = apparent diffusion coefficient; cog-MRGB = cognitive MRGB; fus-MRGB = MRI-TRUS fusion MRGB; inbore-MRGB = in-bore MRGB; MRGB = magnetic resonance–guided biopsy; MRI = magnetic resonance imaging; PCa = prostate cancer; PI-RADS = Prostate Imaging Reporting and Data System; PSA = prostate-specific antigen; T2WI = T2-weighted image; TRUS = transrectal ultrasound.

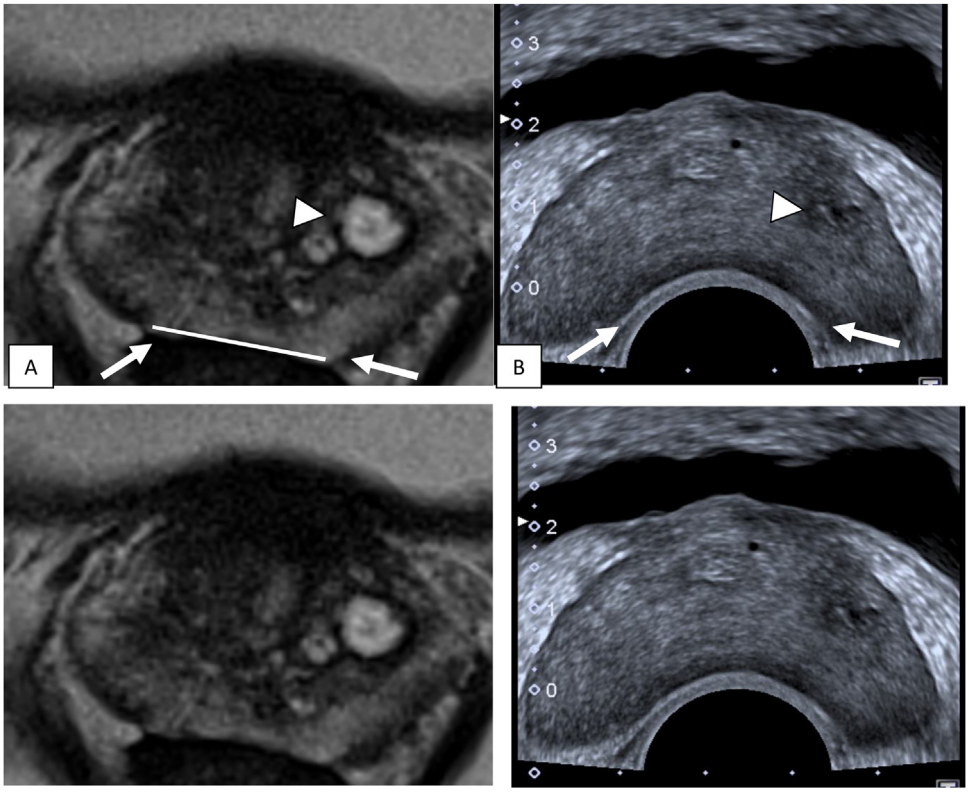

Fig. 4 – Deformation of the prostate by the US probe. A 57-yr-old male (PSA 6.3 ng/ml) with prostate contour—especially PZ—is deformed by the US probe (line in between the white arrows). The cyst (arrowhead) was used as an internal fiducial. The biopsy operator has to retract the US probe a little to release pressure and has to be aware of any mismatch between both images. (A) T2WI uploaded on the US machine. B) US image at corresponding level. PSA = prostate-specific antigen; PZ = peripheral zone; T2WI = T2-weighted image; US = ultrasound.

adequately fuse the different image sets (Fig. 4). Some software packages offer elastic image registration algorithms that allow for surface contour matching by stretching of mpMR images so that these fit the boundaries of the prostate seen on TRUS imaging. Examples of platforms offering such elastic image registration include UroNav (Invivo Corp., Gainesville, FL, USA) and Urostation (Koelis, Grenoble, France) [3,16]. With rigid registration, prostate boundaries are preserved on MRI. Therefore, image registration may be suboptimally aligned despite efforts at alignment. To improve registration and biopsy accuracy, internal fiducials are used for cognitive fusion, as described above (Fig. 1). Biopsee (Pi Medical, Athens, Greece), Smart Fusion (Canon Medical Systems, Otawara, Japan), and Virtual Navigator (Esaote, Genoa, Italy) are examples of software platforms based on rigid image registration [12,17,18]. In Table 1, an overview of the manufacturers of fusion software is shown.

Table 1 – Overview of platforms offering fusion biopsy.

Rigid	Elastic
Virtual Navigator (Esaote)	Urostation (Koelis)
Smart Fusion (Canon Medical Systems)	Artemis (Eigen)
Uronav (Philips/Invivo)	Uronav (Philips/Invivo)
Real-time Virtual Sonography (Hitachi)	
Biopsee (Pi Medical/Medcom)	
Biojet (D&K)	

2.2.1. *Image registration and movement tracking*

Although the different software platforms come with their own specifications and applications, in general, all platforms follow the same procedural steps. First, the prostate mpMR images must be acquired and the lesion must be assessed. In the next step, the prostate outline and suspicious lesions are segmented on mpMRI and uploaded into the ultrasound equipment (often the T2W images). Thereafter, image registration takes place by either contouring the prostate boundaries or using internal fiducials (BPH, cysts, etc.; Fig. 1). Urostation, for example, is a system that requires to delineate the prostate and the suspicious lesion on multiple T2W slices to produce a three-dimensional (3D) volume. This information is then sent to the biopsy machine. After that, the boundaries of the prostate are determined via a sweep of the entire prostate with the TRUS probe. The TRUS-acquired 3D volume of the prostate is then automatically segmented and fused with the MRI-acquired 3D volume.

In our hospital, Smart Fusion (Canon Medical Systems) is used as a TRUS biopsy and fusion platform. The Smart Fusion is a platform that uses rigid image registration software. We import T2W images on the ultrasound machine where they are coupled with the real-time TRUS

images using landmarks seen on both imaging modalities, such as cysts, BPH, or calcifications (Fig. 1). To reduce registration inaccuracies, a landmark as close to the ROI as possible is chosen for image coupling (Fig. 5). After the images are fused, there should be a cognitive enhancement by the operator, who continuously performs mental verifications of the correct orientation of the probe relative to the prostate and ROI.

Movement tracking is done by a small electromagnetically (EM) tracking field generator in combination with a sensor on the ultrasound probe. The EM field generator is placed as close as possible to the ultrasound probe where there is an implanted EM tracking sensor. MR and TRUS images are displayed side by side for cognitive monitoring of the registration and biopsy procedure [19].

An alternative for movement tracking is a mechanical arm or a stepper device. Artemis, for example, uses a mechanical arm that scans the prostate, and tracks the position of the ultrasound probe and the biopsy needle by angle-sensing devices built in the "joints" of the arm [20]. In addition, a mechanical stepper with position sensors is used as a tracking method (Biopsee) [21]. However, Biopsee requires a transperineal biopsy approach. In a recent paper by Marra et al [22], the advantages and disadvantages of a transperineal versus a transrectal biopsy approach is discussed. They concluded that the transperineal biopsy route may offer advantages in terms of infectious-related complications; however, biopsy accuracy and patients' tolerability are comparable.

2.2.2. *Disadvantages and advantages of fus-MRGB*

Compared with cog-MRGB, fus-MRGB is more time consuming and expensive to implement in clinical practice. It requires, at the bedside, expensive coupling software and adequate training to correctly use the MRI-TRUS fusion equipment, as there is a clear learning curve for fus-MRGB. A recent study by Gaziev et al [23] demonstrated a learning curve for fusion biopsy. A total of 340 patients were divided

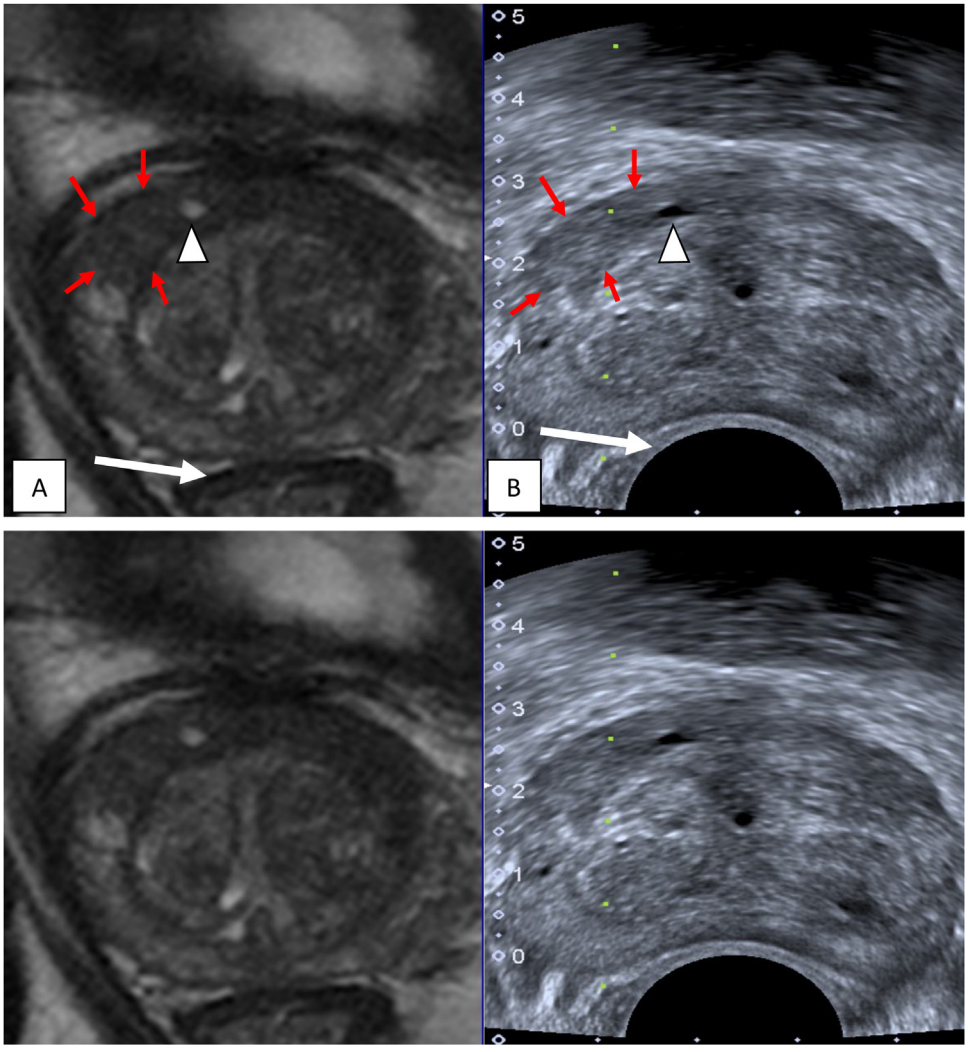

Fig. 5 – Landmark near the suspicious lesion. An 81-yr-old male (PSA 8.3 ng/ml). The cyst is an internal fiducial (arrowhead), as close as possible to the PI-RADS 5 lesion (red arrows; score 5/5/+). This cyst can be used for cognitive fusion after coupling of images in MRI-TRUS fusion. Notice prostate deformation by the US probe (white arrow). Fus-MRGB revealed Gleason 3 + 4. Fus-MRGB = MRI-TRUS fusion MRGB; MRGB = magnetic resonance–guided biopsy; MRI = magnetic resonance imaging; PI-RADS = Prostate Imaging Reporting and Data System; PSA = prostate-specific antigen; TRUS = transrectal ultrasound; US = ultrasound.

in cohorts representing different consecutive time intervals. The prostate cancer detection rate increased from 27% in the first cohort to 63% in the last cohort. In addition, we think that fus-MRGB is less accurate than inbore-MRGB. Unfortunately, publications reporting on the comparison of these techniques are hampered by insufficient study power [5,19]. On the contrary, fus-MRGB seems to be more accurate than cognitive fusion [24,25]. An overview of papers comparing cog-MRGB and fus-MRGB is demonstrated in Table 2.

Additional advantages of fus-MRGB are its relative ease of implementation, lower costs, and less time needed than for the most expensive option, which is inbore-MRGB. Furthermore, just as in cog-MRGB, additional sampling of biopsy cores can be performed in the same session for systematic sampling or to improve targeting accuracy.

2.2.3. Role of fus-MRGB

In our view, fus-MRGB should be the workhorse of prostate biopsy. The advantages of improved detection of csPCa using mpMRI targeted biopsy, better accuracy, and better reliability compared with cog-MRGB, in combination with the advantages of being easy to use in the outpatient setting, make it an ideal first option. Fus-MRGB should be the first step for most suspicious lesions. Different fus-MRGB platforms do not show material differences in the detection of csPCa [14,26,27]. Therefore, costs, usability, and availability should direct the choice between the use of rigid or elastic image registration.

2.3. Direct inbore-MRGB

Inbore-MRGB uses mpMRI visualisation to direct the biopsy needle. Although mpMRI is used both for diagnostics and for needle guidance, acquisition of the diagnostic mpMRI and inbore-MRGB are done in separate sessions. Regardless of improved MRI scanners and fast image acquisition, procedure times are typically in the order of 30–60 min per patient, depending on how many ROIs are biopsied [28].

2.3.1. In-bore MRGB

In our institute, the most frequently used inbore-MRGB approach is transrectal. In special circumstances, for example, in patients who have had an abdominoperineal rectal resection, the transperineal or transgluteal approach can be used. During the biopsy procedure, patients are placed head first and prone in the scanner with a rectally inserted needle guide (Fig. 6). Then, axial T2W images and diffusion-weighted images are obtained to reproduce the previously determined location of the lesion. Using axial and sagittal true fast imaging with steady-state free precession images (TrueFISP), the position of the needle guide can be visualised. To direct the needle towards the suspicious lesion, a physician needs to walk into the MRI scanner room and move the patient partially out of the magnet, in order to (re)adjust the needle guide; after which a new TrueFISP image (Fig. 7) is acquired. This procedure has to be done for several times until the needle guide is placed correctly towards the direction of the suspicious area. To overcome this time-consuming approach, an MR-compatible robotic device named the Remote Controlled Manipulator (Soteria Medical B.V., Arnhem, The Netherlands) has been developed [29,30].

After the needle guide is correctly directed towards the lesion, preferably the part of the lowest apparent diffusion coefficient (ADC) value, the lesion is usually biopsied. At least two 18-gauge needle biopsies are obtained per lesion. With the biopsy needle in situ, a confirmation scan is made to confirm correct needle placement. As the maximum target distance from the tip of the rectal needle guide to an ROI is 5.4 cm, some lesions at the base of very large prostates can be challenging. However, this is rare and can easily be solved by using either a non-MRI compatible biopsy needle (without making a confirmation scan) or the transperineal biopsy approach.

2.3.2. Disadvantages and advantages of inbore-MRGB

Although efforts are made to shorten its procedure time, inbore-MRGB still requires at least 30–60 min per proce-

Table 2 – Overview of studies comparing cognitive and fusion biopsy.

Author	Year of publication	Journal	Conclusion
Delongchamps et al [14]	2013	*Journal of Urology*	Cancer detection rates of rigid and elastic system targeted biopsies were higher than the random biopsy rate. Visual targeted biopsy did not perform better than random biopsy.
Oderda et al [33]	2016	*Urology International*	Fusion biopsies achieve an increased cancer detection rate compared with cognitive biopsies.
Puech et al [12]	2013	*Radiology*	No difference between fusion and cognitive targeted biopsy.
Wysock et al [34]	2014	*European Urology*	Fusion biopsy was more often histologically informative than visual targeting but did not increase cancer detection.
Valerio et al [35]	2015	*Urologic Oncology*	The diagnostic ability of software-based targeted biopsy and visually directed targeted biopsy seems almost comparable, although utility and efficiency both seem to be slightly in favour of the software-based strategy.
Wegelin et al [25]	2017	*European Urology*	No significant advantage of usage of any one technique (fusion, cognitive, or in-bore) for the detection of clinically significant prostate cancer.
Wegelin et al [5]	2019	*European Urology*	No significant difference in the detection of clinically significant prostate cancer among MRGB, fusion, and cognitive biopsy. However, the analyses should be interpreted with caution due to small sample size.

MRGB = magnetic resonance–guided biopsy.

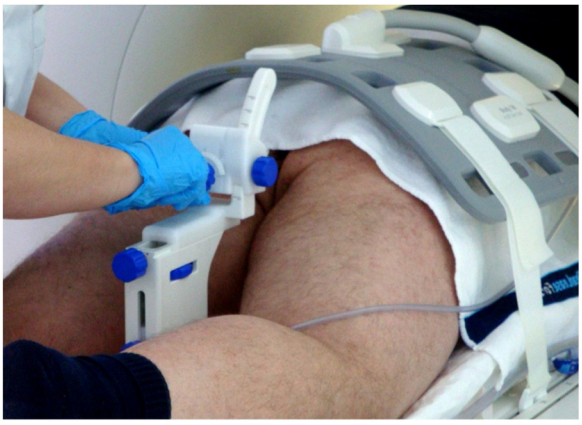

Fig. 6 – Inbore-MRGB. Positioning head first and prone. A dorsal pelvis body phased-array coil is placed. Biopsy device is in between the legs, with rectally inserted needle guide attached. inbore-MRGB = in-bore magnetic resonance–guided biopsy.

dure, depending on how many lesions should be biopsied. On the contrary, fus-MRGB takes only 10–20 min. In the most recent cost-effectiveness study from our hospital, costs for mpMRI and subsequent fus-MRGB or inbore-MRGB were estimated at €800 and €1400, respectively, while TRUS biopsy (without mpMRI) is estimated at €500 [31]. Besides its higher costs, scheduling is an issue. Therefore, not every patient can be offered an inbore-MRGB. In addition, although not reported in literature, there is a clear learning curve for inbore-MRGB.

On the contrary, of the three biopsy methods, inbore-MRGB is likely to be the most accurate approach, as there is no need for image fusion and needle location can be confirmed with direct visibility of the ROI. Unfortunately, publications comparing the three biopsy techniques are not conclusive, due to lack of adequate power [5,19,25].

Furthermore, inbore-MRGB is able to direct the needle towards the area within the suspicious lesion with the lowest ADC value (and likely the most aggressive part in the tumour). This can be important considering the heterogenic nature of prostate cancer [32].

2.3.3. *Role of inbore-MRGB*

Despite the limited availability of inbore-MRGB, it has an important role in the detection of csPCa. In our opinion, inbore-MRGB should be used for selected cases in which fus-MRGB may be more challenging. This is the case, for example, for very small suspicious lesions, and in cases where the coupling system of the fus-MRGB fails (too many calcifications, no available fiducials) or when there is a high clinical suspicion for csPCa, fus- or cog-MRGB is negative or shows insignPCa. In our hospital, the method chosen is discussed in the multidisciplinary team meetings.

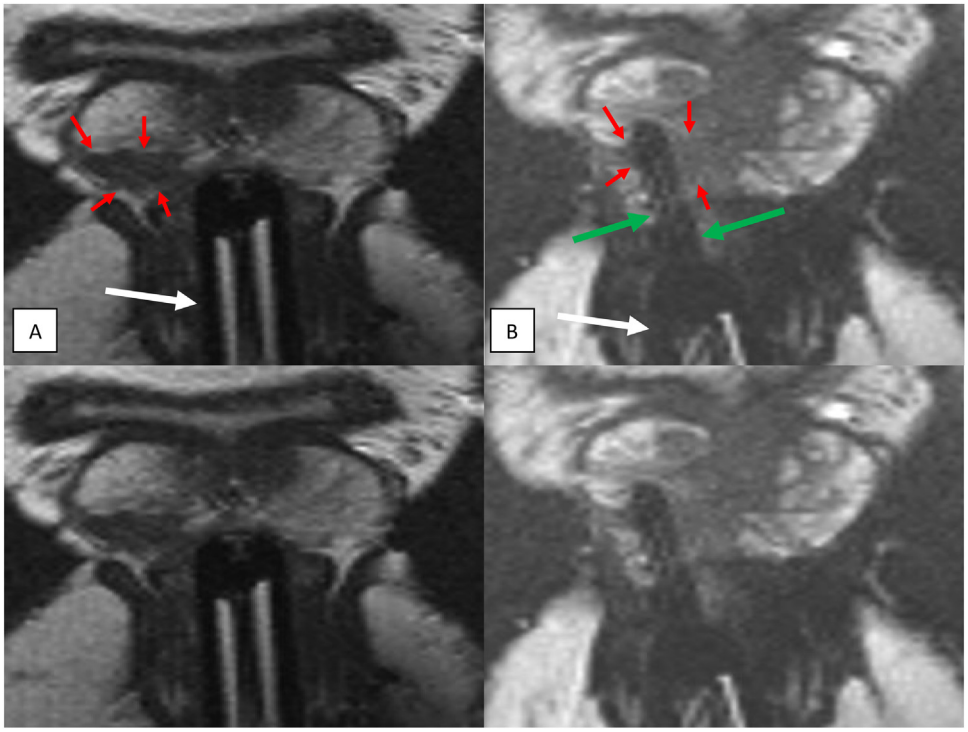

Fig. 7 – Needle positioning in inbore-MRGB. An 80-yr-old male (PSA 9.7 ng/ml). Axial true fast images with steady-state free precession (TrueFISP) for needle positioning. (A) The needle guide (white arrow) is not directing towards the PI-RADS 5 lesion (red arrows; score 5/5/+). To direct the needle towards the suspicious lesion, a physician needs to enter the MRI room, withdraw the patient from the magnet, adjust the needle guide, and make a new TrueFISP image. (B) This has to be done several times until the needle guide is placed correctly in the direction of the lesion. To overcome this time-consuming process, an MR-compatible remote controlled manipulator can be used. The green arrow is showing the biopsy needle within the lesion (red arrows). Pathology revealed Gleason 3 + 4 PCa. inbore-MRGB = in-bore magnetic resonance–guided biopsy; MRI = magnetic resonance imaging; PCa = prostate cancer; PI-RADS = Prostate Imaging Reporting and Data System; PSA = prostate-specific antigen.

3. Conclusions

The previous two "surgery-in-motion" articles and videos addressed the acquisition and interpretation of prostate mpMRI. This paper about MRGB is the last of this triptych. We described the use of cog-MRGB, fus-MRGB, and inbore-MRGB. The (dis)advantages of these biopsy procedures and the proposed role are presented.

To summarise, fus-MRGB is our first choice in prostate biopsy suited for most patients. Direct inbore-MRGB is used in selected, difficult cases and is mainly used as a "problem solver" in patients with a negative fus-MRGB outcome and a persistent high suspicion for csPCa. Cog-MRGB seems to be best for sampling larger lesions and diffuse processes.

***Author contributions*:** Jelle O. Barentsz had full access to all the data in the study and takes responsibility for the integrity of the data and the accuracy of the data analysis.

Study concept and design: Venderink, Bomers, Overduin, de Lauw, Padhani, Sedelaar, Barentsz.
Acquisition of data: Venderink, Bomers, Barentsz.
Analysis and interpretation of data: Venderink, Bomers, Overduin, de Lauw, Padhani, Sedelaar, Barentsz.
Drafting of the manuscript: Venderink, Bomers, Barentsz.
Critical revision of the manuscript for important intellectual content: Venderink, Bomers, Overduin, de Lauw, Padhani, Sedelaar, Barentsz.
Statistical analysis: Venderink, Bomers, Overduin, de Lauw, Padhani, Sedelaar, Barentsz.
Obtaining funding: None.
Administrative, technical, or material support: Venderink, Bomers, Barentsz.
Supervision: Barentsz.
Other: None.

Financial disclosures: Jelle O. Barentsz certifies that all conflicts of interest, including specific financial interests and relationships and affiliations relevant to the subject matter or materials discussed in the manuscript (eg, employment/affiliation, grants or funding, consultancies, honoraria, stock ownership or options, expert testimony, royalties, or patents filed, received, or pending), are the following: None.

***Funding/Support and role of the sponsor*:** This work was supported by Soteria Medical.

Acknowledgements: We would like to thank Soteria Medical (Arnhem, NL) for their assistance in producing the video.

Appendix A. Supplementary data

Supplementary material related to this article can be found, in the online version, at doi:https://doi.org/10.1016/j.eururo.2019.10.009.

References

[1] Ahmed HU, El-Shater Bosaily A, Brown LC, et al. Diagnostic accuracy of multi-parametric MRI and TRUS biopsy in prostate cancer (PROMIS): a paired validating confirmatory study. Lancet 2017;389:815–22.
[2] Kasivisvanathan V, Rannikko AS, Borghi M, et al. MRI-targeted or standard biopsy for prostate-cancer diagnosis. N Engl J Med 2018;378:1767–77.
[3] Siddiqui MM, Rais-Bahrami S, Turkbey B, et al. Comparison of MR/ultrasound fusion-guided biopsy with ultrasound-guided biopsy for the diagnosis of prostate cancer. JAMA 2015;313:390–7.
[4] van der Leest M, Cornel E, Israel B, et al. Head-to-head comparison of transrectal ultrasound-guided prostate biopsy versus multiparametric prostate resonance imaging with subsequent magnetic resonance-guided biopsy in biopsy-naive men with elevated prostate-specific antigen: a large prospective multicenter clinical study. Eur Urol 2019;75:570–8.
[5] Wegelin O, Exterkate L, van der Leest M, et al. The FUTURE trial: a multicenter randomised controlled trial on target biopsy techniques based on magnetic resonance imaging in the diagnosis of prostate cancer in patients with prior negative biopsies. Eur Urol 2019;75:582–90.
[6] Schouten MG, van der Leest M, Pokorny M, et al. Why and where do we miss significant prostate cancer with multi-parametric magnetic resonance imaging followed by magnetic resonance-guided and transrectal ultrasound-guided biopsy in biopsy-naive men? Eur Urol 2017;71:896–903.
[7] Kwak JT, Hong CW, Pinto PA, et al. Is visual registration equivalent to semiautomated registration in prostate biopsy? Biomed Res Int 2015;2015:394742.
[8] Abd-Alazeez M, Kirkham A, Ahmed HU, et al. Performance of multiparametric MRI in men at risk of prostate cancer before the first biopsy: a paired validating cohort study using template prostate mapping biopsies as the reference standard. Prostate Cancer Prostatic Dis 2014;17:40–6.
[9] Futterer JJ, Briganti A, De Visschere P, et al. Can clinically significant prostate cancer be detected with multiparametric magnetic resonance imaging? A systematic review of the literature. Eur Urol 2015;68:1045–53.
[10] Haffner J, Lemaitre L, Puech P, et al. Role of magnetic resonance imaging before initial biopsy: comparison of magnetic resonance imaging-targeted and systematic biopsy for significant prostate cancer detection. BJU Int 2011;108(8 Pt 2):E171–8.
[11] Park BK, Park JW, Park SY, et al. Prospective evaluation of 3-T MRI performed before initial transrectal ultrasound-guided prostate biopsy in patients with high prostate-specific antigen and no previous biopsy. AJR Am J Roentgenol 2011;197:W876–81.
[12] Puech P, Rouviere O, Renard-Penna R, et al. Prostate cancer diagnosis: multiparametric MR-targeted biopsy with cognitive and transrectal US-MR fusion guidance versus systematic biopsy—prospective multicenter study. Radiology 2013;268:461–9.
[13] Tonttila PP, Lantto J, Paakko E, et al. Prebiopsy multiparametric magnetic resonance imaging for prostate cancer diagnosis in biopsy-naive men with suspected prostate cancer based on elevated prostate-specific antigen values: results from a randomized prospective blinded controlled trial. Eur Urol 2016;69:419–25.
[14] Delongchamps NB, Peyromaure M, Schull A, et al. Prebiopsy magnetic resonance imaging and prostate cancer detection: comparison of random and targeted biopsies. J Urol 2013;189:493–9.
[15] Logan JK, Rais-Bahrami S, Turkbey B, et al. Current status of magnetic resonance imaging (MRI) and ultrasonography fusion software platforms for guidance of prostate biopsies. BJU Int 2014;114:641–52.
[16] Rud E, Baco E, Eggesbo HB. MRI and ultrasound-guided prostate biopsy using soft image fusion. Anticancer Res 2012;32:3383–9.
[17] van de Ven WJ, Venderink W, Sedelaar JP, et al. MR-targeted TRUS prostate biopsy using local reference augmentation: initial experience. Int Urol Nephrol 2016;48:1037–45.
[18] Hadaschik BA, Kuru TH, Tulea C, et al. A novel stereotactic prostate biopsy system integrating pre-interventional magnetic resonance imaging and live ultrasound fusion. J Urol 2011;186:2214–20.

[19] Venderink W, van der Leest M, van Luijtelaar A, et al. Retrospective comparison of direct in-bore magnetic resonance imaging (MRI)-guided biopsy and fusion-guided biopsy in patients with MRI lesions which are likely or highly likely to be clinically significant prostate cancer. World J Urol 2017;35:1849–55.

[20] Marks L, Young S, Natarajan S. MRI-ultrasound fusion for guidance of targeted prostate biopsy. Curr Opin Urol 2013;23:43–50.

[21] Kuru TH, Roethke MC, Seidenader J, et al. Critical evaluation of magnetic resonance imaging targeted, transrectal ultrasound guided transperineal fusion biopsy for detection of prostate cancer. J Urol 2013;190:1380–6.

[22] Marra G, Ploussard G, Futterer J, Valerio M, Party E-YPCW. Controversies in MR targeted biopsy: alone or combined, cognitive versus software-based fusion, transrectal versus transperineal approach? World J Urol 2019;37:277–87.

[23] Gaziev G, Wadhwa K, Barrett T, et al. Defining the learning curve for multiparametric magnetic resonance imaging (MRI) of the prostate using MRI-transrectal ultrasonography (TRUS) fusion-guided transperineal prostate biopsies as a validation tool. BJU Int 2016;117:80–6.

[24] Cool DW, Zhang X, Romagnoli C, Izawa JI, Romano WM, Fenster A. Evaluation of MRI-TRUS fusion versus cognitive registration accuracy for MRI-targeted, TRUS-guided prostate biopsy. AJR Am J Roentgenol 2015;204:83–91.

[25] Wegelin O, van Melick HHE, Hooft L, et al. Comparing three different techniques for magnetic resonance imaging-targeted prostate biopsies: a systematic review of in-bore versus magnetic resonance imaging-transrectal ultrasound fusion versus cognitive registration. Is there a preferred technique? Eur Urol 2017;71:517–31.

[26] Gayet M, van der Aa A, Beerlage HP, Schrier BP, Mulders PF, Wijkstra H. The value of magnetic resonance imaging and ultrasonography (MRI/US)-fusion biopsy platforms in prostate cancer detection: a systematic review. BJU Int 2016;117:392–400.

[27] Venderink W, de Rooij M, Sedelaar JPM, Huisman HJ, Futterer JJ. Elastic versus rigid image registration in magnetic resonance imaging-transrectal ultrasound fusion prostate biopsy: a systematic review and meta-analysis. Eur Urol Focus 2018;4:219–27.

[28] Overduin CG, Futterer JJ, Barentsz JO. MRI-guided biopsy for prostate cancer detection: a systematic review of current clinical results. Curr Urol Rep 2013;14:209–13.

[29] Bomers JG, Bosboom DG, Tigelaar GH, Sabisch J, Futterer JJ, Yakar D. Feasibility of a 2(nd) generation MR-compatible manipulator for transrectal prostate biopsy guidance. Eur Radiol 2017;27:1776–82.

[30] Zamecnik P, Schouten MG, Krafft AJ, et al. Automated real-time needle-guide tracking for fast 3-T MR-guided transrectal prostate biopsy: a feasibility study. Radiology 2014;273:879–86.

[31] Venderink W, Govers TM, de Rooij M, Futterer JJ, Sedelaar JPM. Cost-effectiveness comparison of imaging-guided prostate biopsy techniques: systematic transrectal ultrasound, direct in-bore MRI, and image fusion. AJR Am J Roentgenol 2017;208:1058–63.

[32] Hambrock T, Hoeks C, Hulsbergen-van de Kaa C, et al. Prospective assessment of prostate cancer aggressiveness using 3-T diffusion-weighted magnetic resonance imaging-guided biopsies versus a systematic 10-core transrectal ultrasound prostate biopsy cohort. Eur Urol 2012;61:177–84.

[33] Oderda M, Faletti R, Battisti G, et al. Prostate cancer detection rate with Koelis fusion biopsies versus cognitive biopsies: a comparative study. Urol Int 2016;97:230–7.

[34] Wysock JS, Rosenkrantz AB, Huang WC, et al. A prospective, blinded comparison of magnetic resonance (MR) imaging-ultrasound fusion and visual estimation in the performance of MR-targeted prostate biopsy: the PROFUS trial. Eur Urol 2014;66:343–51.

[35] Valerio M, McCartan N, Freeman A, Punwani S, Emberton M, Ahmed HU. Visually directed vs. software-based targeted biopsy compared to transperineal template mapping biopsy in the detection of clinically significant prostate cancer. Urol Oncol 2015;33(424):e429–416.

[36] Engels RRM, Israël B, Padhani AR, Barentsz JO. Multiparametric magnetic resonance imaging for the detection of clinically significant prostate cancer: what urologists need to know. Part 1: acquisition. Eur Urol 2020;77:457–68.

[37] Israël B, van der Leest M, Sedelaar JPM , et al. Multiparametric magnetic resonance imaging for the detection of clinically significant prostate cancer: what urologists need to know. Part 2: interpretation. Eur Urol 2020;77:469–80.